

**DIRECTED PERCOLATION AND
OTHER SYSTEMS WITH ABSORBING STATES:
IMPACT OF BOUNDARIES**

PER FRÖJDH*

*Department of Physics, Stockholm University
Box 6730, S-113 85 Stockholm, Sweden*

MARTIN HOWARD†

*Department of Physics, Simon Fraser University
Burnaby, British Columbia, Canada V5A 1S6*

KENT BÆKGAARD LAURITSEN‡

*Atmosphere Ionosphere Research Division
Danish Meteorological Institute, 2100 Copenhagen, Denmark*

Received (received date)

Revised (revised date)

We review the critical behavior of nonequilibrium systems, such as directed percolation (DP) and branching-annihilating random walks (BARW), which possess phase transitions into absorbing states. After reviewing the bulk scaling behavior of these models, we devote the main part of this review to analyzing the impact of walls on their critical behavior. We discuss the possible boundary universality classes for the DP and BARW models, which can be described by a general scaling theory which allows for two independent surface exponents in addition to the bulk critical exponents. Above the upper critical dimension d_c , we review the use of mean field theories, whereas in the regime $d < d_c$, where fluctuations are important, we examine the application of field theoretic methods. Of particular interest is the situation in $d = 1$, which has been extensively investigated using numerical simulations and series expansions. Although DP and BARW fit into the same scaling theory, they can still show very different surface behavior: for DP some exponents are degenerate, a property not shared with the BARW model. Moreover, a “hidden” duality symmetry of BARW in $d = 1$ is broken by the boundary and this relates exponents and boundary conditions in an intricate way.

Keywords: Phase transitions; Nonequilibrium systems; Absorbing states; Directed percolation; Branching-annihilating random walks; Surface and bulk critical behavior.

*email: frojdh@physto.se

†email: mjhoward@sfu.ca

‡email: kbl@dmi.dk

1. Introduction

As is well known from the study of equilibrium statistical mechanics, boundaries have important effects on systems close to criticality.^{1,2,3} Quantities measured close to a wall can scale differently than in the bulk where, for a given bulk universality class, various boundary universality classes are possible. An analysis of the effects of boundaries is clearly very important if one wishes to apply the theory of critical phenomena to real physical systems. Although the theory of equilibrium surface critical phenomena is now well understood, the equivalent theory for nonequilibrium systems is in a much less advanced state. It is the purpose of this review to describe recent progress in extending the theory of surface critical phenomena to certain nonequilibrium problems.

The most prominent example of such a nonequilibrium dynamic system is directed percolation (DP), which is the generic model for systems with a continuous phase transition from an active to an absorbing state from which the system cannot escape. DP describes the directed growth of a cluster (i.e. growth in a preferred spatial direction or along the time axis), where the growth rate is governed by a microscopic growth probability p . For probabilities below a critical value, $p < p_c$, the cluster will die after a finite time, which means that the system gets trapped in the vacuum—the unique empty state. On the other hand, for high enough growth probabilities $p > p_c$, there is a finite probability that the cluster will always remain active. Exactly at $p = p_c$, there is a critical phase transition from the active into the absorbing state.⁴ A whole range of systems possessing a phase transition from a non-trivial active phase into a unique absorbing state fall into this universality class. Some examples include epidemics, chemical reactions, interface pinning/depinning, the contact process, polynuclear growth, and certain cellular automata.^{5,6}

Although most models with absorbing states fall into the ubiquitous DP universality class, there are important exceptions. For instance, the model of *branching-annihilating random walks* with an even number of offspring (BARW) exhibits quite different behavior^{7,8,9} and defines a separate universality class. Other models in this class (at least in one spatial dimension, $d = 1$) include certain probabilistic cellular automata,¹⁰ monomer-dimer models,^{11,12,13} non-equilibrium kinetic Ising models,¹⁴ and generalized DP with two absorbing states (DP2).¹⁵ These models escape from the DP universality class by possessing an extra conservation law or symmetry: for the BARW model, a “parity” conservation of the total number of particles modulo 2; for the other models, an underlying symmetry between their absorbing states. Models with an infinite number of absorbing states are believed to belong to the BARW class if the absorbing states can be arranged into two symmetric groups (see Ref. 13 and references therein). On the other hand, if no higher symmetries between the absorbing states are present, then such models will belong to the DP class.

In the present review we focus our attention on the impact of walls on systems

with nonequilibrium critical phase transitions into absorbing states.^{16,17,18,19,20,21,22,23,24,25,26,27,28} We will describe the boundary critical behavior of DP and BARW by using a variety of methods, including mean field theory, scaling theory, field theory, exact calculations, Monte-Carlo simulations, and series expansions. The rest of this review is organized as follows: In Section 2 we introduce percolation and reaction-diffusion models for DP and BARW for bulk systems (without boundaries). Then in Section 3 we quickly review the general bulk scaling behavior of such systems. In Section 4 we briefly discuss the surface critical behavior of equilibrium systems, with a particular emphasis on the semi-infinite Ising model. In Section 5 we then introduce walls into our nonequilibrium models and discuss in detail some possible boundary conditions in $d = 1$. In Sections 6, 7, 8, and 9 we review the various theoretical techniques used to analyze the surface critical behavior of our nonequilibrium models, including mean field, scaling, and field theories and also exact calculations. In Section 10 we present results for critical exponents based on numerical work. In Section 11 we review recent work in other directions concerning surfaces in DP-like systems. Finally we give a summary and outlook in Section 12.

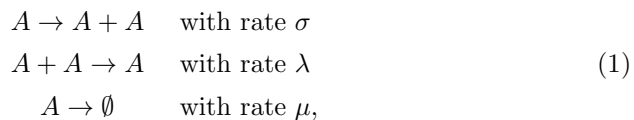
2. Bulk DP and BARW

In this section we introduce the models for DP and BARW. We describe both reaction-diffusion versions of these models as well as the probabilistic cellular automata frequently used in simulations in $d = 1$.

2.1. DP

The easiest way of introducing DP is to consider bond percolation on a directed lattice. The update rules for bond DP in d spatial dimensions are then easily defined: for each site at time t , form bonds with probability p to the neighboring sites at time $t + 1$.⁴

As is well known, various reaction-diffusion models also fall into the DP universality class.^{29,30,31} The simplest of these is defined by the following reaction scheme:



where the identical particles A otherwise perform simple random walks with diffusion constant D .

In $d = 1$, the DP universality class has also frequently been studied by using the Domany-Kinzel model.^{32,33} In this cellular automata model each site can either be active or inactive and the probability for site i to be updated to state $s_{i,t+1}$ at time $t + 1$ is given by an update probability $P(s_{i,t+1}|s_{i-1,t}, s_{i+1,t})$. See Figure 1 for a typical lattice configuration and Figure 2 for the update rules. An example of a cluster grown from a single seed according to these rules is shown in Figure 3a.

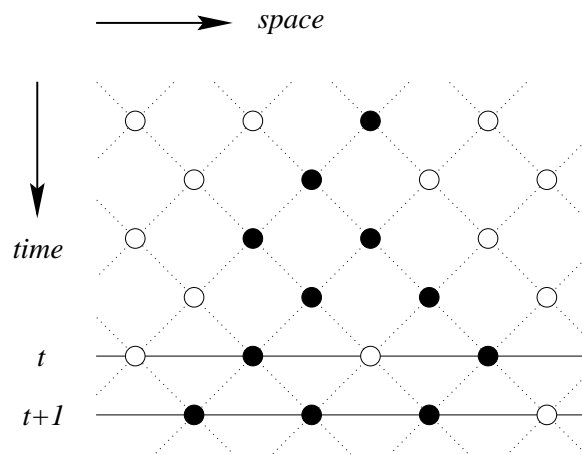


Fig. 1. Directed Percolation in terms of the Domany-Kinzel model, where time flows vertically downwards. Black sites are active (A) and white ones inactive (I). The state of each site at time $t + 1$ depends on the states of the neighboring sites at time t .

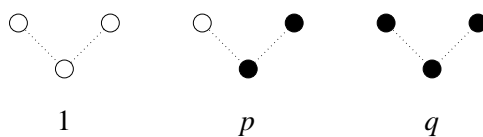


Fig. 2. Update probabilities for DP in terms of the parameters $0 \leq p, q \leq 1$, where we have $q = p(2 - p)$ for bond DP and $q = p$ for site DP, respectively. Probabilities for the other configurations follow from left-right symmetry and from $P(A | \dots) + P(I | \dots) = 1$.

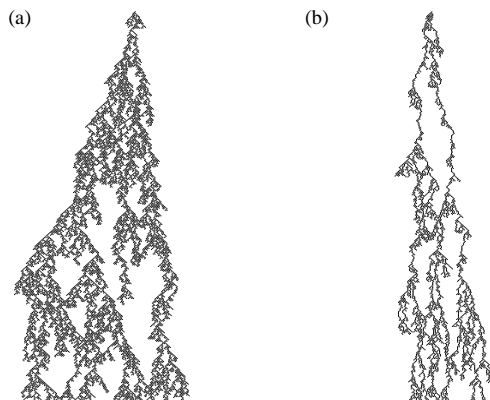
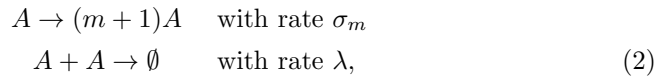


Fig. 3. (a) A DP cluster and (b) a DP2 cluster both grown from a single seed in the bulk.

2.2. BARW

The BARW model is defined by a reaction-diffusion system, with the following reaction processes^{7,8,9}



where the identical particles A otherwise perform simple random walks with diffusion constant D . For m odd, the above model is known to belong to the DP universality class, however for m even we have what we refer to as the BARW universality class. Unless otherwise specified when we refer to the BARW model we will be referring to the even m case.

The BARW class has also been studied in $d = 1$ using a generalized Domany-Kinzel model (sometimes called $DPn^{21,27}$) introduced by Hinrichsen.¹⁵ In this model each site can be either active or in one of n inactive states. For $n = 1$ the update rules are identical to those of the Domany-Kinzel model in Figure 2, but for $n \geq 2$, the distinction between regions of different inactive states is preserved by demanding that they are separated by active ones. An example of a DP2 cluster is shown in Figure 3b. The DP2 model has two symmetric absorbing states in which the system can become trapped. The update probabilities for $d = 1$, where DP2 is known to belong to the BARW universality class,¹⁵ are given in Figure 4.

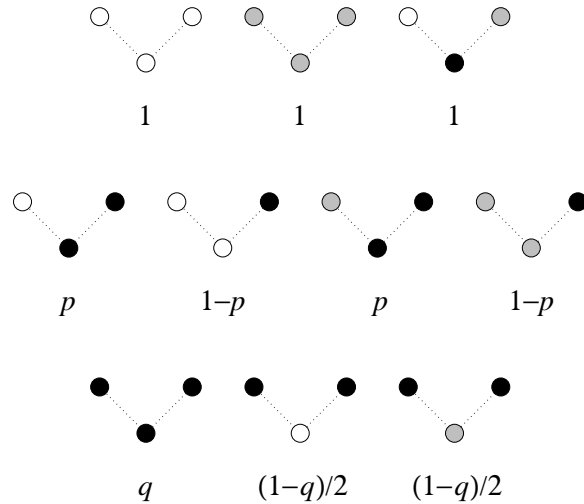


Fig. 4. Update probabilities for DP2: black sites are active (A), whereas white and grey sites are in the inactive states I_1 and I_2 , respectively. Probabilities for the other configurations follow from left-right symmetry and from $P(A | \dots) + P(I_1 | \dots) + P(I_2 | \dots) = 1$.

3. Bulk Scaling

The growth of both DP and BARW clusters in the bulk close to criticality can be summarized by a set of independent exponents. A natural choice is to consider ν_{\perp} and ν_{\parallel} which describe the divergence of the correlation lengths in space,

$$\xi_{\perp} \sim |\Delta|^{-\nu_{\perp}}, \quad (3)$$

and time

$$\xi_{\parallel} \sim |\Delta|^{-\nu_{\parallel}}. \quad (4)$$

Here the parameter Δ describes the deviation from the critical point. For DP and DPn, $\Delta = p_c - p$, whereas for the reaction-diffusion models in mean field theory $\Delta = \mu - \sigma$ for DP, and $\Delta = -m\sigma_m$ for BARW. We also need the order parameter exponent β , which can be defined in two *a priori* different ways: it is either governed by the percolation probability (the probability that a cluster grown from a finite seed never dies),

$$P(t \rightarrow \infty, \Delta) \sim |\Delta|^{\beta_{\text{seed}}}, \quad \Delta < 0, \quad (5)$$

or by the coarse-grained density of active sites in the steady state,

$$n(\Delta) \sim |\Delta|^{\beta_{\text{dens}}}, \quad \Delta < 0. \quad (6)$$

When $\Delta < 0$ the system is said to be in an *active* state, whereas for $\Delta = 0$ the system is *critical* (with an algebraically decaying density), and for $\Delta > 0$ (if applicable) the system is either *inactive* (DP) or again critical (BARW).³⁴ For the case of DP, it is known that β is unique: $\beta_{\text{seed}} = \beta_{\text{dens}}$ in any dimension, both above and below the upper critical dimension $d_c = 4$. This follows from time-reversal symmetry²³ and field theoretic considerations^{35,29} and has been verified by extensive numerical work. The relation also holds for BARW in $d = 1$, a result first suggested by numerics and now backed up by an exact duality mapping.³⁶ However, this exponent equality is certainly not always true: if we consider the BARW mean field regime valid for spatial dimensions $d > d_c = 2$, then the system is in a critical inactive state only for a zero branching rate, where the density decays away as a power law. However, any nonzero branching rate results in an active state, with a nonzero steady state density⁹ (see Figure 5a). As the branching rate is reduced towards zero, this density (6) approaches zero continuously with the mean field exponent $\beta_{\text{dens}} = 1$. Nevertheless, for $d > 2$, the survival probability (5) of a particle cluster will be finite for *any* value of the branching rate, implying that $\beta_{\text{seed}} = 0$ in mean-field theory. This result follows from the non-recurrence of random walks in $d > 2$.

Field theoretically, DP is believed to be satisfactorily understood—the appropriate field theory^{29,31} (sometimes called Reggeon Field Theory, see Section 8.1) is well under control and the exponents have been computed to two loop order in an $\epsilon = 4 - d$ expansion.³⁰ However, for the case of BARW (see Section 8.2), a description of the $d = 1$ case poses considerable difficulties for the field theory.⁹ These stem

from the presence of two critical dimensions: $d_c = 2$ (above which mean-field theory applies) and $d'_c \approx 4/3$. For $d > d'_c$ the behavior of Figure 5a holds, i.e. an active state results for *any* nonzero value of the branching σ_m , whereas for $d < d'_c$ the system is only active for $\sigma_m > \sigma_{m,\text{critical}}$,⁹ as shown in Figure 5b. This means that the physical spatial dimension $d = 1$ cannot be accessed using controlled perturbative expansions down from the upper critical dimension $d_c = 2$. Furthermore, for the $\sigma_m < \sigma_{m,\text{critical}}$ region, the system is *not* inactive (in the sense of an exponentially decaying density). Instead this entire phase is controlled by the annihilation fixed point of the $A + A \rightarrow \emptyset$ process, where the density decays away as a power law. Hence this phase should rather be considered as still being critical.

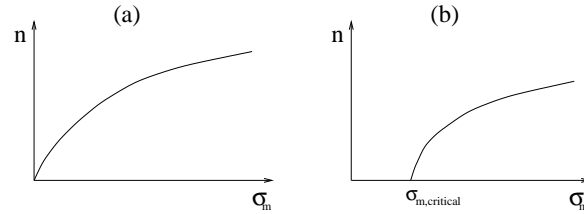


Fig. 5. Schematic bulk behavior for BARW of the density n as a function of the branching rate σ_m for (a) $d \geq 2$ and (b) $d = 1$.

Despite the problems associated with BARW for $d < d'_c$, we can still put forward a general scaling theory for DP and BARW, valid both above and below their critical dimensions. However, we must retain a possible distinction between β_{seed} and β_{dens} . For example, the average lifetime $\langle t \rangle$ of finite clusters can be derived from the scaling form for the survival probability

$$P(t, \Delta) = |\Delta|^{\beta_{\text{seed}}} \varphi(t/\xi_{\parallel}). \quad (7)$$

We then find

$$\langle t \rangle = \int t P(t, \Delta) dt \sim |\Delta|^{-\tau}, \quad (8)$$

where

$$\tau = \nu_{\parallel} - \beta_{\text{seed}}. \quad (9)$$

The appropriate scaling form for the density $n(\mathbf{x}, t)$, given that the cluster was started at $\mathbf{x} = \mathbf{0}, t = 0$, is

$$n(x, t, \Delta) = |\Delta|^{\beta_{\text{seed}} + \beta_{\text{dens}}} f(x/\xi_{\perp}, t/\xi_{\parallel}). \quad (10)$$

Notice that rotational symmetry about the seeding point $\mathbf{x} = \mathbf{0}$ implies that the spatial coordinates enter the scaling function only as $x = |\mathbf{x}|$, the distance from the seeding point. Using the expression (10) we see that the average mass of finite clusters scales as

$$\langle s \rangle = \int n(x, t, \Delta) d^d x dt \sim |\Delta|^{-\gamma} \quad (11)$$

where γ is related to the other exponents via the following hyperscaling relation:

$$\nu_{\parallel} + d\nu_{\perp} = \beta_{\text{seed}} + \beta_{\text{dens}} + \gamma. \tag{12}$$

Note that Eq. (12) is consistent with the distinct upper critical dimensions for BARW and DP. Using the above mean field values for BARW and $\nu_{\perp} = 1/2$, $\nu_{\parallel} = 1$, and $\gamma = 1$, we verify $d_c = 2$. In contrast, for DP one has the mean-field exponents $\beta_{\text{dens}} = \beta_{\text{seed}} = 1$, $\gamma = 1$, and $d_c = 4$. In Tables 1 and 2 we list the exponents for DP (see Refs. 17,37,38,39,40,41,42,43,44 and references therein) and BARW (see Refs. 15,45,46 and references therein).

Table 1. Critical exponents for DP.

	$d = 1$	$d = 2$	$d = 3$	Mean Field
$\beta_{\text{dens}} = \beta_{\text{seed}}$	0.276 486(8)	0.583(4)	0.805(10)	1
ν_{\parallel}	1.733 847(6)	1.295(6)	1.105(5)	1
ν_{\perp}	1.096 854(4)	0.733(4)	0.581(5)	1/2
τ	1.457 362(14)	0.711(7)	0.298(12)	0
γ	2.277 730(5)	1.593(7)	1.232(12)	1

Table 2. Critical exponents for BARW.

	$d = 1$	Mean Field
β_{dens}	0.922(5)	1
β_{seed}	0.93(5)	0
ν_{\parallel}	3.22(3)	1
ν_{\perp}	1.84(2)	1/2
τ	2.30(3)	1
γ	3.22(3)	1

4. Equilibrium Surface Critical Behavior

We will begin our discussion of boundaries in critical systems by briefly reviewing the theory of surface critical phenomena for equilibrium systems,³ with particular emphasis on the Ising model. Defined on a half space, the semi-infinite Ising model serves as the canonical example of a system exhibiting surface critical behavior.

Each bulk Ising spin has the same number $2d$ of nearest neighbors. However, by cutting the lattice in half, spins next to the wall possess fewer neighbors than those in the bulk and are therefore more weakly coupled. At high temperatures T , the system is disordered and thus correlations are short ranged. Hence the effects of the wall are localized to a thin layer along the wall and decay away exponentially into the bulk with a length scale governed by the bulk correlation length. However, as the temperature is lowered the system will become critical at $T = T_c$, the critical temperature of the infinite system. At this point, where the correlation length diverges, the decay of the perturbation introduced by the wall is algebraic, and hence the impact of the wall on the scaling behavior is very marked. The two-point spin-spin correlation function decays with a new exponent along the wall,

independent of the two exponents required to describe bulk Ising criticality. In this case, the critical behavior of the surface is referred to as the *ordinary transition*. In two dimensions, the boundary critical exponent governing the decay of the two point correlation function is known exactly.⁴⁷

We could also imagine replacing all the spin couplings at the wall by stronger ones than in the bulk. Starting from the disordered state and lowering T , we will now have a situation where the strongly coupled wall spins may potentially undergo a phase transition already at $T > T_c$. In this case, the wall spins order independently of the bulk which remains disordered at this temperature. Of course, if the boundary is of sufficiently low dimension (e.g. the one dimensional boundary of a semi-infinite $2d$ Ising model) then such ordering cannot occur at finite temperatures. But, for $d = 3$, the surface is two dimensional and in these circumstances can undergo a so called *surface transition*. This surface transition (if it exists) lies in the same universality class as a $d - 1$ dimensional bulk transition. By further reducing the temperature, the bulk will then order at $T = T_c$ in the presence of an already ordered surface. In this case, the critical behavior of the boundary is referred to as the *extraordinary transition*. This is quite different to the ordinary transition discussed above, where the surface was compelled to order through its coupling to the ordered bulk. At the extraordinary transition, where $T = T_c$, the system is again critical, but the correlations close to the wall differ from the case of the ordinary transition, and are governed by another independent boundary critical exponent.

In principle we may tune the wall couplings such that the boundary transition takes place at $T = T_c$. Another name for this point where the bulk and boundary transitions coincide is the *special transition*. It is a multicritical point and connects the lines of ordinary, extraordinary and surface critical points in the phase diagram of bulk and wall couplings.

For $d = 2$ the surface and special transitions cannot take place, since the surface is one-dimensional. However, an alternative way of ordering the surface layer is to introduce a magnetic field that only couples to wall spins. The boundary phase transition at $T = T_c$ in the presence of such a field is called a *normal transition*. It turns out that the exact mechanism responsible for ordering the wall is unimportant, and thus the normal transition is in fact equivalent to the extraordinary transition.⁴⁸ Hence, in two dimensions, we only need to distinguish between two universality classes. These can be accessed using the following boundary conditions: a free (open) boundary will give an ordinary transition and a fixed boundary will give an extraordinary transition. For both cases, the corresponding exponents are exactly known. Even the four-point functions governing the universal cross-over from wall to bulk correlations are exactly known from conformal field theory.⁴⁹

Another interesting aspect of the Ising model is the Kramers-Wannier duality, which is a mapping of the Ising model from disorder to order and vice versa.⁵⁰ The self dual point defines T_c . However, by introducing a surface, the self-duality at $T = T_c$ is broken and it is straightforward to show that under the duality open boundaries are mapped to fixed boundaries and vice versa. Hence, the duality now

maps the two boundary universality classes onto one another. This observation is useful to bear in mind when analyzing the BARW model, where we will see that a self-duality broken by the wall again relates boundary universality classes in a subtle way.

5. DP and BARW with Walls

We now turn our attention to an understanding of the boundary critical properties of the nonequilibrium DP and BARW models. We will begin by detailing the boundary conditions of these models.

For the reaction-diffusion version of DP, the modification is simple, we simply allow for the DP reactions (1) to occur at (potentially) different rates on the surface as compared to their values in the bulk. By tuning these boundary reaction rates, we can access the various boundary universality classes, in a similar way as was achieved in the Ising model by tuning the surface spin couplings.

For the case of BARW, the situation is a little more complicated. The basic idea is that on the surface we may include not only the usual branching and annihilation reactions (2) but potentially also a parity symmetry breaking $A \rightarrow \emptyset$ reaction. Depending on whether or not the $A \rightarrow \emptyset$ reaction is actually present, we may then expect different boundary universality classes according to whether the symmetry of the bulk is broken or respected at the surface. We note that a somewhat similar situation in an equilibrium system has recently been analyzed in Ref. 51.

For the case of the $d = 1$ cellular automata introduced in Section 2, there are several obvious boundary conditions. The simplest is just to cut off the lattice. This is equivalent to introducing boundary sites which are forced to be in one of the inactive states. We will refer to this case as the inactive boundary condition (IBC), and, for DP2, we choose inactivity of type 1 to the left of the boundary, see Figure 6. Apart from imposing the state of these sites within the wall, the sites at the wall and those in the bulk are updated by the rules in Figures 2 and 4.

Next we consider the reflecting boundary condition (RBC) where the wall acts like a mirror so that the sites within the wall are always a mirror image of those next to the wall, see Figure 7. For DP2, one can see that there is a qualitative difference between the IBC and the RBC. For the latter, regions of type-2 inactivity can get trapped at the wall and the only way for these regions to disappear is to wait for the cluster to return. On the other hand, for the IBC, such regions are never trapped.

A third type of boundary condition is the active boundary condition (ABC) where the sites within the wall are forced to be active, see Figure 8. In this case the cluster will never die completely as the wall will always be active and can always induce new clusters.

Although it is not readily apparent, it turns out that these three boundary conditions exhaust all possible boundary universality classes for the BARW model in $d = 1$. We will return later in Sections 6.3.2 and 6.3.4 to the question of which boundary universality class is to be associated with each of the IBC, RBC, and ABC boundary conditions.

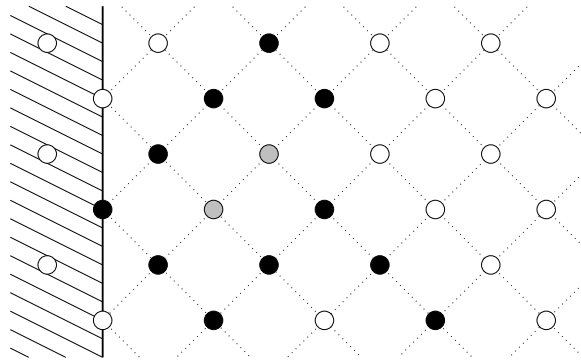


Fig. 6. DP2 with an inactive boundary condition (IBC).

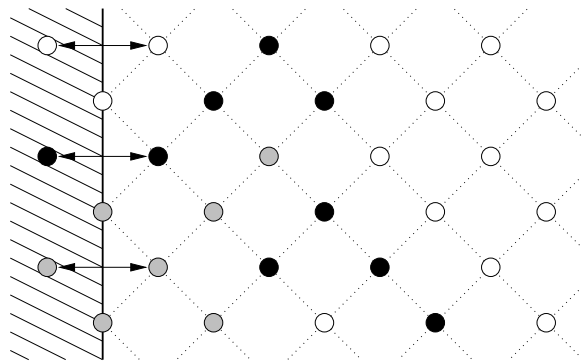


Fig. 7. DP2 with a reflecting boundary condition (RBC).

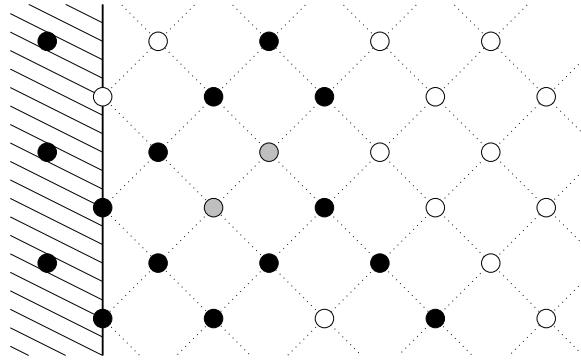


Fig. 8. DP2 with an active boundary condition (ABC).

6. Boundary Critical Behavior of DP and BARW

6.1. Surface DP

First of all, let us examine the effects of introducing a $d - 1$ dimensional wall at $x_{\perp} = 0$ [$\mathbf{x} = (\mathbf{x}_{\parallel}, x_{\perp})$] into a DP process. Note that the labels parallel (\parallel) and perpendicular (\perp) refer here to directions relative to the wall (and not relative to the time direction). An example of such a cluster grown close to a wall is shown in Figure 9b.

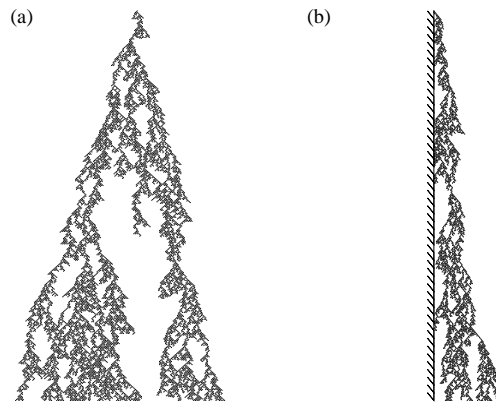


Fig. 9. DP clusters in the Domany-Kinzel model grown from a single seed (a) in the bulk and (b) next to an impenetrable wall.

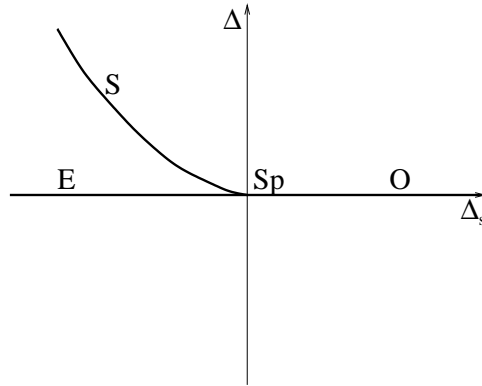


Fig. 10. Schematic mean field phase diagram for boundary DP. The transitions are labeled by O=ordinary, E=extraordinary, S=surface, and Sp=special.

Following on from our discussion of boundaries in equilibrium systems (see Section 4), it is not difficult to justify a schematic phase diagram for boundary DP (see Figure 10 and also Ref. 16). In Figure 10, Δ and Δ_s represent, respectively, the deviations of the bulk and surface from criticality. For $\Delta_s > 0$ and as $\Delta \rightarrow 0$, we see an ordinary transition, since in that case we expect the bulk to order in a situation where the boundary, if isolated, would be disordered. On the other hand, for $\Delta > 0$ and for Δ_s sufficiently negative, we expect the boundary to order even while the bulk is disordered, i.e. the surface transition. Then for $\Delta_s < 0$ and $\Delta \rightarrow 0$, the bulk will order in the presence of an already ordered boundary, i.e. an extraordinary transition for the boundary. Finally at $\Delta = \Delta_s = 0$, where all the critical lines meet, and where both the bulk and isolated surface would be critical, we expect a multicritical point, i.e. the special transition.

The bulk exponents are, of course, unchanged by the presence of a surface and, furthermore, one can show that the correlation length exponents on the boundary are also the same as in the bulk.^{2,16} In the following, for conciseness, we will concentrate solely on the ordinary transition; more details on some of the other transitions can be found in Refs. 16,27. At the ordinary transition, one finds just *one* extra independent exponent associated with the boundary: this can be taken to be the surface density exponent $\beta_{1,\text{dens}}$. This is defined from the steady-state density at the wall, where we have

$$n(x_{\perp} = 0, \Delta) \sim |\Delta|^{\beta_{1,\text{dens}}^{\text{O}}}, \quad \Delta < 0. \quad (13)$$

In principle one could also allow for a second type of surface β_1 exponent, one defined from a survival probability for clusters started on the wall

$$P_1(t \rightarrow \infty, \Delta) \sim |\Delta|^{\beta_{1,\text{seed}}^{\text{O}}}, \quad \Delta < 0. \quad (14)$$

However, the surface exponents here show a similar pattern to their bulk counterparts and fulfill $\beta_{1,\text{seed}}^{\text{O}} = \beta_{1,\text{dens}}^{\text{O}} = \beta_1^{\text{O}}$, as can be shown using a time-reversal

symmetry argument (cf. Ref. 23) or by a field-theoretic derivation of an appropriate correlation function (see Section 8.1 and also Ref. 19).

6.1.1. Mean field theory for surface DP

In this section, we very briefly review some simple results for boundary DP at the mean field level, focusing again on the ordinary transition. A more general analysis can be found in Ref. 27 (see also Appendix C of Ref. 24). The equation describing mean field DP with a surface is

$$\partial_t n = D\nabla^2 n - \Delta n - \lambda n^2, \quad (15)$$

with the boundary condition

$$D\partial_{x_\perp} n|_{x_\perp=0} = \Delta_s n|_{x_\perp=0}. \quad (16)$$

Here the variable $\Delta = \mu - \sigma$ is the difference between the rates for the $A \rightarrow \emptyset$ and $A \rightarrow A + A$ processes. Similarly we have the surface variable Δ_s , and the bulk quadratic term is due to the reaction $A + A \rightarrow A$. From the above Eq. (15), the bulk mean field exponents can easily be computed: $\nu_\parallel = 1$, $\nu_\perp = 1/2$, and $\beta = 1$. Furthermore, with the inclusion of a boundary, we see that the correlation length exponents are unchanged at the wall but the surface β_1 exponents are altered. If we are interested in the mean field steady state, then we can replace Eq. (15) with

$$Dn'' - \Delta n - \lambda n^2 = 0, \quad (17)$$

where $n'' \equiv d^2 n/dx_\perp^2$. The appropriate boundary condition (16) is given by

$$Dn'_s = \Delta_s n_s, \quad (18)$$

where $n_s = n|_{x_\perp=0}$, and $n'_s = dn/dx_\perp|_{x_\perp=0}$. Multiplying Eq. (17) by n' and integrating, we have

$$\frac{1}{2}Dn'^2 - \frac{1}{2}\Delta n^2 - \frac{1}{3}\lambda n^3 + C = 0, \quad (19)$$

where C is a constant of integration. Using the bulk results $n' = 0$, and $n = (-\Delta)/\lambda$ for $\Delta < 0$, or $n = 0$ for $\Delta > 0$, we have

$$\frac{\Delta_s n_s}{D} = - \left[\frac{\lambda}{D} \right]^{1/2} \left(n_s - \frac{|\Delta|}{\lambda} \right) \left(\frac{2}{3}n_s + \frac{|\Delta|}{3\lambda} \right)^{1/2} \quad [\Delta < 0] \quad (20)$$

$$\frac{\Delta_s n_s}{D} = - \left[\frac{\lambda}{D} \right]^{1/2} n_s \left(\frac{2}{3}n_s + \frac{\Delta}{\lambda} \right)^{1/2} \quad [\Delta > 0] \quad (21)$$

where we have also used the boundary condition (18). Considering the ordinary transition where $\Delta_s > 0$ and $\Delta \rightarrow 0^-$, we expect $n = |\Delta|/\lambda \gg n_s$, and thus Eq. (20) yields $n_s \propto |\Delta|^{3/2}$, giving the mean field value $\beta_1^O = 3/2$.

6.2. Surface BARW

For the case of BARW, we expect a similar picture to hold as that described for DP in Section 6.1. In particular, the expressions (13) and (14) for the steady state density and survival probabilities will also apply. However, unlike DP, we will see that the $\beta_{1,\text{seed}}$ and $\beta_{1,\text{dens}}$ exponents are no longer equal.

6.2.1. Mean field theory for surface BARW

The surface phase diagram for the mean field theory of BARW (valid for $d > d_c = 2$) is shown in Figure 11. Here σ_m , σ_{m_s} are the rates for the branching processes $A \rightarrow (m+1)A$ in the bulk and at the surface, respectively, and μ_s is the rate for the surface spontaneous annihilation reaction $A \rightarrow \emptyset$. Otherwise, the labeling is the same as that for the DP phase diagram (see Figure 10). We summarize the main details of the phase diagram below; more details can be found in Ref. 27.

The first feature to note is that the bulk is either active ($\sigma_m > 0$) or critical ($\sigma_m = 0$), but never inactive. Hence, unlike DP, there is no possibility of finding a surface transition, where the surface is critical with the bulk inactive. For the case where $\sigma_m = \mu_s = 0$, we expect that for any finite value of the surface branching, the surface will become active. This corresponds to the extraordinary transition with an active surface and critical bulk. On the other hand for $\sigma_m = \sigma_{m_s} = 0$ and $\mu_s > 0$, the density at an (isolated) surface would decay away exponentially quickly due to the $A \rightarrow \emptyset$ reaction, and hence we have the ordinary transition. Consequently with $\sigma_m = 0$, but both μ_s and σ_{m_s} non-zero, there should be a line of special transitions dividing the extraordinary and ordinary regions. This explains the general features of the phase diagram in Figure 11.

At a more quantitative level, the mean field equation for BARW is very similar to that for DP:

$$\partial_t n = D\nabla^2 n - \Delta n - \lambda n^2, \quad (22)$$

with the boundary condition

$$D\partial_{x_\perp} n|_{x_\perp=0} = \Delta_s n|_{x_\perp=0}. \quad (23)$$

However the values of the Δ , Δ_s parameters are now different: $\Delta = -m\sigma_m$ and $\Delta_s = -m\sigma_{m_s} + \mu_s$. For simplicity we will again focus only on the ordinary transition (details of the other transitions can be found in Ref. 27). Clearly we expect the same mean field exponent $\beta_{1,\text{dens}}$ as in DP.⁵² However, the mean field behavior of the $\beta_{1,\text{seed}}$ exponent is very different from the corresponding behavior in DP. Consider placing two particles next to the surface at $t = 0$. From the recurrence properties of random walks we see that, regardless of the reaction rates on the surface or in the bulk, there is a finite chance that the two particles will never meet again. Hence the survival probability is *nonzero* and thus $\beta_{1,\text{seed}}^O = 0$ in mean field theory.

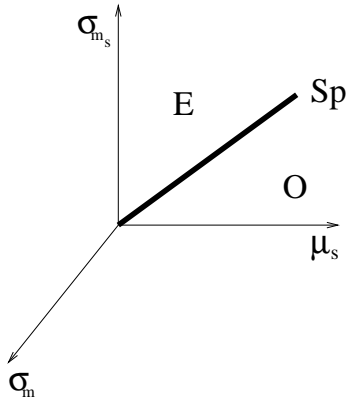


Fig. 11. Schematic mean field boundary phase diagram for BARW. See text for an explanation of the labeling.

6.3. Beyond mean field theory

6.3.1. Surface DP

We expect that the phase diagram shown in Figure 10 is generally valid for surface DP close to the upper critical dimension $d_c = 4$. However, as first pointed out in Ref. 27, in $d = 1$, where the surface is just a zero dimensional point, the phase diagram may look rather different. In that case, for an inactive bulk, net particle production is only possible at one point. Furthermore, since particles will be constantly lost into the bulk, where they will decay away exponentially quickly, it may not be possible to form an active surface state. Of course this conclusion assumes the absence of a surface reaction $\emptyset \rightarrow A$, which is the analog of a surface magnetic field in the Ising model. If this reaction is included then a normal transition obviously becomes possible.

6.3.2. Boundary condition classification for $d = 1$ DP cellular automata

Following the analysis in the previous section, we can now attempt to assign universality classes for the IBC, RBC, ABC cellular automata boundary conditions introduced earlier in Section 5. The ABC condition obviously behaves as if there existed a surface reaction equivalent to $\emptyset \rightarrow A$, and thus it belongs to the normal transition universality class. Numerically, the IBC, RBC, belong to the same universality class,²¹ which we identify as the ordinary transition.

6.3.3. Surface BARW

Next we turn our attention to the $d = 1$ phase diagram for surface BARW shown in Figure 12. The phase diagram looks quite different from its mean field analog due in part to the shift of the bulk critical point away from zero branching rate, but

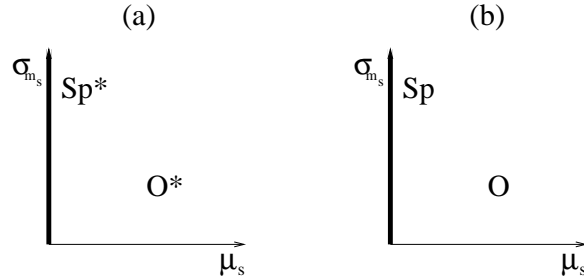


Fig. 12. Schematic surface phase diagrams for BARW in $d = 1$ for (a) $\sigma_m < \sigma_{m,\text{critical}}$, and (b) $\sigma_m = \sigma_{m,\text{critical}}$. See text for an explanation of the labeling.

also due to the absence of any extraordinary transition. Again, in the absence of the surface reactions of the form $\emptyset \rightarrow A$, this is due to the fact that excess particle production (with a finite reaction rate) at a zero dimensional surface is simply not efficient enough to generate an active state, due to leakage into the critical bulk.

We now divide the phase diagram into two sections, as in Figure 12.

$\sigma_m < \sigma_{m,\text{critical}}$:

In this case, the bulk will be controlled by the annihilation process $A + A \rightarrow \emptyset$, and the branching process will be everywhere irrelevant. Consider first the case with $\mu_s = 0$, where the surface reaction $A \rightarrow \emptyset$ is not permitted. In that case, since both the wall and bulk will be controlled by the critical $A + A \rightarrow \emptyset$ reaction, we expect an analog of the special transition. However, this will not be a special transition in the usual sense, since in this region it will *not* be possible to obtain an active state either on the surface or in the bulk by small changes in the bulk and/or surface branching rates. To emphasize this point, we label this regime as Sp^* in Figure 12a. This simpler and analytically tractable case has already been extensively analyzed in Ref. 26 (see also Section 8.3). Next we consider the case $\mu_s > 0$, where the reaction $A \rightarrow \emptyset$ is permitted on the wall. Since the branching is irrelevant in this region of parameter space, the reaction $A \rightarrow \emptyset$ would give rise to an exponentially decaying density at an isolated boundary, and hence an inactive state. Consequently we expect an analog of the ordinary transition. However, for the same reasons as described above, we will label this regime as O^* in Figure 12a.

$\sigma_m = \sigma_{m,\text{critical}}$:

Since we are now at the bulk critical point, which borders the bulk active phase, we expect rather different behavior to that described above. In this case it *will* be possible to obtain an active bulk/surface state by small changes in the reaction parameters. For the case where $\mu_s = 0$, with both the bulk and surface critical, we

expect a standard special transition (labeled as Sp in Figure 12b). On the other hand, if $\mu_s > 0$, then the parity symmetry of BARW is broken at the boundary and we expect a critical bulk and (if isolated) an inactive surface, i.e. a standard ordinary transition (labeled as O in Figure 12b).

6.3.4. *Boundary condition classification for $d = 1$ BARW cellular automata*

We can now discuss the relations between the boundary conditions for the $d = 1$ DP2 cellular automata introduced in Section 5 and our above classification of the boundary universality classes for BARW in $d = 1$. The key feature is whether the symmetry in DP2 between the two absorbing states in the bulk is preserved at the surface. This symmetry is the analog of the parity symmetry conservation in the reaction-diffusion BARW model, which allows the DP universality class to be escaped. As we discussed above, breaking the parity symmetry on the boundary leads to the ordinary transition. The analog of that situation is provided by the RBC model which breaks the symmetry between the absorbing states on the boundary and hence also belongs to the ordinary transition. On the other hand, the IBC model respects the symmetry at the boundary, and thus belongs to the special transition. Furthermore, the ABC model once again clearly belongs to the normal transition universality class. Hence, as claimed earlier in Section 5, we see that by using the IBC, RBC, ABC classification all the previously discussed boundary BARW transitions in $d = 1$ can be accessed.

7. Scaling Theory

In this section we review the scaling theory for the survival probabilities and correlation functions for boundary DP and BARW. For simplicity we again restrict ourselves to the ordinary transition; additional details can be found in Refs. 19,21,27.

7.1. *Surface DP*

As we mentioned in Section 6.1, the most important point to emphasize is that there is only one boundary β_1^O exponent for DP: $\beta_1^O = \beta_{1,\text{seed}}^O = \beta_{1,\text{dens}}^O$. The survival probability (the probability that the cluster is still alive at time t) has the form

$$P_1(t, \Delta) = \Delta^{\beta_1^O} \psi_1(t/\xi_{\parallel}), \quad (24)$$

where the scaling function ψ_1 is constant for $t \gg \xi_{\parallel}$.³⁵ The mean lifetime of finite clusters

$$\langle t \rangle \sim |\Delta|^{-\tau_1^O} \quad (25)$$

then follows from the lifetime distribution $-dP_1/dt$,¹⁷ yielding the exponent

$$\tau_1^O = \nu_{\parallel} - \beta_1^O. \quad (26)$$

However, for $\nu_{\parallel} < \beta_1^O$, the leading contribution to $\langle t \rangle$ will be a constant, such that the above scaling relation breaks down and is replaced by $\tau_1 = 0$.

For the coarse-grained bulk density n_1 at the point (\mathbf{x}, t) of a cluster grown from a single seed located next to the wall at $\mathbf{x} = \mathbf{0}$, $t = 0$, one can make the scaling ansatz

$$n_1(x, t, \Delta) = \Delta^{\beta_1^O + \beta} f_1(x/\xi_\perp, t/\xi_\parallel). \quad (27)$$

This ansatz may be properly justified using the field theory analysis reviewed in Section 8.1, however a more intuitive justification of the prefactors may be given as follows. The first factor of $\Delta^{\beta_1^O}$ comes from the probability that an infinite cluster can be grown from the seed. The second factor of Δ^β arises from the bulk scaling of activity in the active state, i.e., the (conditional) probability that the point (\mathbf{x}, t) belongs to the infinite cluster grown from the seed (see also Ref. 28). In contrast, if the density is measured at the wall, then the appropriate ansatz reads

$$n_{11}(x, t, \Delta) = \Delta^{2\beta_1^O} f_{11}(x/\xi_\perp, t/\xi_\parallel), \quad (28)$$

as we pick up a factor $\Delta^{\beta_1^O}$ rather than Δ^β for the probability that (\mathbf{x}, t) at the wall belongs to the infinite cluster grown from the seed.

By integrating the cluster density (27) over space and time, we arrive at the average size of finite clusters grown from seeds on the wall,

$$\langle s \rangle \sim |\Delta|^{-\gamma_1^O}, \quad (29)$$

such that

$$\nu_\parallel + d\nu_\perp = \beta_1^O + \beta + \gamma_1^O. \quad (30)$$

Hence, the surface exponent γ_1 is related to the previously defined exponents via a scaling law that naturally generalizes the usual $d + 1$ dimensional bulk hyperscaling relation

$$\nu_\parallel + d\nu_\perp = 2\beta + \gamma. \quad (31)$$

The results of numerical simulations with a wall (see Section 10) are in very good agreement with the hyperscaling relation (30).

Besides integrating the density (27), we can also integrate the density on the wall (28) over the $d - 1$ dimensional wall and time. This integration yields the average (finite) cluster size on the wall,

$$\langle s_{1,1} \rangle \sim |\Delta|^{-\gamma_{1,1}^O}, \quad (32)$$

where

$$\nu_\parallel + (d - 1)\nu_\perp = 2\beta_1^O + \gamma_{1,1}^O. \quad (33)$$

However, in higher dimensions ($d \approx 2$ being a marginal case) this relation is not fulfilled as it would predict a negative $\gamma_{1,1}^O$. For this case, $\gamma_{1,1}^O = 0$, reflecting a constant contribution to Eq. (32), cf. the comment after Eq. (26).

7.2. Edge DP

We next turn to briefly review the case of DP clusters started on an edge. It has been known for some time that the presence of an edge introduces new exponents, independent of those associated with the bulk or with a surface (see Ref. 53 for a discussion in the context of equilibrium critical phenomena, or Ref. 28 in the context of percolation).

Consider a system, where we allow the wall to have an edge with an angle α at $x_{\parallel}^{(1)} = x_{\perp} = 0$. Hence, the edge is simply the $d - 2$ dimensional intersection of two $d - 1$ dimensional walls. By placing the seed next to this edge, the boundary exponent β_1^O is replaced by the edge exponent $\beta_2^O(\alpha)$ (where of course $\beta_1^O = \beta_2^O(\pi)$). Following the same arguments as before, we have the new scaling ansatz for the cluster density

$$n_2(r, t, \Delta) = \Delta^{\beta_2^O + \beta} f_2(r/\xi_{\perp}, t/\xi_{\parallel}), \quad (34)$$

where r is the radial coordinate in a system of spherical polar coordinates centered on $x_{\parallel}^{(1)} = x_{\perp} = 0$. This ansatz applies for directions away from the edge and the walls. By replacing β with β_1^O or β_2^O , we get the corresponding results for the density along the wall or the edge, respectively. Moreover, in analogy with Eqs. (29) and (30) for seeds on a wall, we obtain the average (finite) size $\langle s \rangle \sim |\Delta|^{-\gamma_2^O}$ of clusters grown from a seed next to an edge, by integrating Eq. (34) over space and time. This yields the hyperscaling relation

$$\nu_{\parallel} + d\nu_{\perp} = \beta_2^O + \beta + \gamma_2^O. \quad (35)$$

Quoting the results from Ref. 19 for a mean field calculation of the edge exponents

$$\gamma_2^O = 1 - \pi/2\alpha, \quad \beta_2^O = 1 + \pi/2\alpha, \quad (36)$$

we see that Eq. (35) is satisfied at the upper critical dimension $d_c = 4$. Numerical estimates for the exponent β_2^O from Ref. 19, together with the mean field values, are listed in Table 3 (see Section 10 for further details on simulation methods).

Table 3. Numerical estimates for the β_2^O exponents for edge DP together with the mean field values from Eq. (36). Recall that $\beta_2^O(\pi) = \beta_1^O$. The bulk and $d = 1$ wall estimates are listed for reference.

Angle (α)	$\pi/2$	$3\pi/4$	π	$5\pi/4$	bulk
β_1^O ($d = 1$)			0.73371(2)		0.276486(8)
β_2^O ($d = 2$)	1.6(1)	1.23(7)	1.07(5)	0.98(5)	0.583(4)
β_2^O (MF)	2	5/3	3/2	7/5	1

7.3. Surface BARW

In this section we briefly review the analogous scaling theory for surface BARW. Again, for brevity, we will only consider the ordinary transition. When writing down

this scaling theory we must now bear in mind the important distinction between the $\beta_{1,\text{dens}}$ and $\beta_{1,\text{seed}}$ exponents. For a seed placed on the wall at $\mathbf{x} = \mathbf{0}$, $t = 0$, the scaling form for the survival probability has the form

$$P_1(t, \Delta) = |\Delta|^{\beta_{1,\text{seed}}^{\text{O}}} \Phi_1(t/\xi_{\parallel}). \quad (37)$$

It is then straightforward to compute the average lifetime of finite clusters, $\langle t \rangle \sim |\Delta|^{-\tau_1}$, where $\tau_1^{\text{O}} = \nu_{\parallel} - \beta_{1,\text{seed}}^{\text{O}}$, just as in the case of DP.

For the coarse-grained bulk particle density n_1 at the point (\mathbf{x}, t) of a cluster grown from a single seed located next to the wall at $\mathbf{x} = \mathbf{0}$, $t = 0$, one can make the ansatz

$$n_1(x, t, \Delta) = |\Delta|^{\beta_{1,\text{seed}}^{\text{O}} + \beta_{\text{dens}}} g_1(x/\xi_{\perp}, t/\xi_{\parallel}). \quad (38)$$

As was the case for DP, the Δ -prefactor in Eq. (38) comes from Eq. (37) for the probability that an infinite cluster can be grown from the seed, and from Eq. (6) for the (conditional) probability that the point (\mathbf{x}, t) belongs to this cluster. If, instead, the density is measured at the wall, we have

$$n_{11}(x, t, \Delta) = |\Delta|^{\beta_{1,\text{seed}}^{\text{O}} + \beta_{1,\text{dens}}^{\text{O}}} g_{11}(x/\xi_{\perp}, t/\xi_{\parallel}), \quad (39)$$

as we pick up a factor $|\Delta|^{\beta_{1,\text{dens}}^{\text{O}}}$ rather than $|\Delta|^{\beta_{\text{dens}}}$ from the probability that (\mathbf{x}, t) at the wall belongs to the cluster. The average size of finite clusters

$$\langle s_1 \rangle \sim |\Delta|^{-\gamma_1^{\text{O}}}, \quad (40)$$

follows from integrating the cluster density (38) over space and time, where the exponent γ_1^{O} is related to the previously defined exponents via

$$\nu_{\parallel} + d\nu_{\perp} = \beta_{1,\text{seed}}^{\text{O}} + \beta_{\text{dens}} + \gamma_1^{\text{O}}. \quad (41)$$

Analogously, by integrating the cluster wall density (39) over the $(d-1)$ -dimensional wall and time, we obtain the average size of finite clusters on the wall

$$\langle s_{1,1} \rangle \sim |\Delta|^{-\gamma_{1,1}^{\text{O}}}, \quad (42)$$

where

$$\nu_{\parallel} + (d-1)\nu_{\perp} = \beta_{1,\text{seed}}^{\text{O}} + \beta_{1,\text{dens}}^{\text{O}} + \gamma_{1,1}^{\text{O}}. \quad (43)$$

Note that if the γ exponents obtained from Eqs. (41) and (43) are negative, then they should be replaced by zero in Eqs. (40) and (42).

8. Field Theory

In the following sections we briefly review the available field theoretic results for bulk and boundary^{16,27} DP and BARW. These techniques allow for the systematic inclusion of fluctuation effects, important below the upper critical dimension d_c .

8.1. DP field theory

The field theory describing bulk DP is very well known.^{29,31} The action is given by

$$S_{\text{bulk}} = \int d^d x \int dt \left(\bar{\phi} [\partial_t - D\nabla^2 + \Delta] \phi + \frac{1}{2} u [\bar{\phi} \phi^2 - \bar{\phi}^2 \phi] \right), \quad (44)$$

where $\phi(\mathbf{x}, t)$ is the “density” field, and where $\bar{\phi}(\mathbf{x}, t)$ is the response field. Simple power counting reveals that the upper critical dimension is $d_c = 4$ below which fluctuation effects become important. Renormalization of the theory is standard, involving field, mass (Δ), diffusion constant (D) and coupling constant (u) renormalizations. The critical exponents can then be computed perturbatively using an $\epsilon = 4 - d$ expansion, giving³⁰

$$\beta_{\text{seed}} = \beta_{\text{dens}} = 1 - \frac{\epsilon}{6} + O(\epsilon^2), \quad \nu_{\parallel} = 1 + \frac{\epsilon}{12} + O(\epsilon^2), \quad \nu_{\perp} = \frac{1}{2} + \frac{\epsilon}{16} + O(\epsilon^2). \quad (45)$$

Note that, in this case, the exponents β_{seed} and β_{dens} can be shown to be equal. Technically, this follows from the fact that the density and response fields renormalize identically (see also Ref. 54).

In the action (44) one can integrate out the response field $\bar{\phi}(\mathbf{x}, t)$ and arrive at a Langevin equation for the local density $\phi(\mathbf{x}, t)$:

$$\frac{\partial \phi(\mathbf{x}, t)}{\partial t} = D\nabla^2 \phi(\mathbf{x}, t) - \Delta \phi(\mathbf{x}, t) - \frac{1}{2} u \phi(\mathbf{x}, t)^2 + \eta(\mathbf{x}, t), \quad (46)$$

with

$$\langle \eta(\mathbf{x}, t) \rangle = 0, \quad \langle \eta(\mathbf{x}, t) \eta(\mathbf{x}', t') \rangle = u \phi(\mathbf{x}, t) \delta^d(\mathbf{x} - \mathbf{x}') \delta(t - t'), \quad (47)$$

where $\eta(\mathbf{x}, t)$ is a Gaussian noise term. The multiplicative factor $\phi(\mathbf{x}, t)$ in the noise correlator reflects the fact that $\phi = 0$ is the absorbing state.

The use of field theories to study boundary nonequilibrium phase transitions was initiated by Janssen et al.¹⁶ They showed that the appropriate action for DP with a wall at $x_{\perp} = 0$ is given by $S = S_{\text{bulk}} + S_{\text{surface}}$, where

$$S_{\text{surface}} = \int d^{d-1} x \int dt \Delta_s \bar{\phi}_s \phi_s, \quad (48)$$

with the definitions $\phi_s = \phi(\mathbf{x}_{\parallel}, x_{\perp} = 0, t)$ and $\bar{\phi}_s = \bar{\phi}(\mathbf{x}_{\parallel}, x_{\perp} = 0, t)$. The surface term S_{surface} corresponds to the most relevant interaction consistent with the symmetries of the problem and which also respects the absorbing state condition. Simple power counting indicates that $[\Delta_s] \sim \kappa$, where κ denotes an inverse length scale. The presence of the wall implies the boundary condition at $x_{\perp} = 0$ of

$$D\partial_{x_{\perp}} \phi|_s = \Delta_s \phi_s. \quad (49)$$

Using this boundary condition, we see that a boundary term of the form $\bar{\phi}_s \partial_{x_{\perp}} \phi_s$, although marginal from power counting arguments, is actually redundant.

Since $\Delta_s \sim \kappa$, its renormalized value can only flow to one of three possible fixed points: 0 or $\pm\infty$. These possibilities correspond to the various types of boundary

phase transitions. The flow $\Delta_s \rightarrow -\infty$ (∞) corresponds to the extraordinary (ordinary) transition, whereas the unstable fixed point at $\Delta_s = 0$ corresponds to the multicritical special transition. In the following we will concentrate solely on the ordinary transition, since that is the only case to have been studied numerically (see Ref. 16 for a field theoretic analysis of the special transition).

The only extra renormalization required by the presence of the wall is a surface field renormalization.¹⁶ The presence of this extra renormalization at the surface leads naturally to the existence of just one independent surface exponent β_1^O . Once again, the exponents $\beta_{1,\text{seed}}^O$ and $\beta_{1,\text{dens}}^O$ can be shown to be equal¹⁹ $\beta_{1,\text{seed}}^O = \beta_{1,\text{dens}}^O = \beta_1^O$, similar to the result found in the bulk. This follows from the fact that the *surface* density and response fields renormalize identically. Furthermore it can be shown that the correlation length exponents are everywhere unchanged by the wall (see Refs. 2,16). The β_1^O exponent can again be computed using an $\epsilon = 4 - d$ expansion yielding¹⁶

$$\beta_1^O = \beta_{1,\text{seed}}^O = \beta_{1,\text{dens}}^O = \frac{3}{2} - \frac{7\epsilon}{48} + O(\epsilon^2). \quad (50)$$

From the field theory of Ref. 16, it is not hard to verify that Eq. (30) is the appropriate generalization of Eq. (31), relating β_1^O to

$$\gamma_1^O = \frac{1}{2} + \frac{7\epsilon}{48} + O(\epsilon^2). \quad (51)$$

8.2. BARW field theory

We now briefly review the bulk field theory for the BARW reaction-diffusion system. In order to properly include fluctuation effects for BARW, one must be careful to include processes generated by a combination of branching and annihilation. In other words in addition to the process $A \rightarrow (m+1)A$, the reactions $A \rightarrow (m-1)A$, \dots , $A \rightarrow 3A$ need to be included. These considerations lead to the full action⁹

$$\begin{aligned} S_{\text{bulk}}[\psi, \hat{\psi}; \tau] = & \int d^d x \left[\int_0^\tau dt \left(\hat{\psi}(\mathbf{x}, t) [\partial_t - D\nabla^2] \psi(\mathbf{x}, t) \right. \right. \\ & + \sum_{l=1}^{m/2} \sigma_{2l} [1 - \hat{\psi}(\mathbf{x}, t)^{2l}] \hat{\psi}(\mathbf{x}, t) \psi(\mathbf{x}, t) \\ & \left. \left. - \lambda [1 - \hat{\psi}(\mathbf{x}, t)^2] \psi(\mathbf{x}, t)^2 \right) - \psi(\mathbf{x}, \tau) - n_0 \hat{\psi}(\mathbf{x}, 0) \right], \end{aligned} \quad (52)$$

written in terms of the response field $\hat{\psi}(\mathbf{x}, t)$ and the “density” field $\psi(\mathbf{x}, t)$. Here D is the diffusion constant, λ the annihilation rate, and σ_{2l} the branching rate for the process $A \rightarrow (2l+1)A$. Note that the final two terms in Eq. (52) represent, respectively, a contribution due to the projection state (see Ref. 55), and the initial condition (an uncorrelated Poisson distribution with mean n_0). Notice also that (for *even* m) the action (52) is invariant under the “parity” transformation

$$\hat{\psi}(\mathbf{x}, t) \rightarrow -\hat{\psi}(\mathbf{x}, t), \quad \psi(\mathbf{x}, t) \rightarrow -\psi(\mathbf{x}, t). \quad (53)$$

This symmetry corresponds physically to particle conservation modulo 2 and it enables the system to escape the DP universality class.

Simple power counting on the action in Eq. (52) reveals that the upper critical dimension is $d_c = 2$. Close to d_c , the renormalization of the above action is quite straightforward (here we again quote the results from Ref. 9). At the annihilation fixed point the RG eigenvalue of the branching parameter can easily be computed. To one loop order one finds $y_{\mu_m} = 2 - m(m+1)\epsilon/2 + O(\epsilon^2)$, where $\epsilon = 2 - d$. Hence we see that the *lowest* branching process is actually the most relevant. Therefore, close to 2 dimensions, where the branching remains relevant, we expect to find an *active* state for all nonzero values of the branching (as was the case for the BARW mean field theory reviewed earlier).

However, inspection of the above most relevant RG eigenvalue y_{σ_2} shows that it eventually becomes negative at $d = d'_c \approx 4/3$. In that case we expect a major change in the behavior of the system, since the branching process will no longer be relevant at the annihilation fixed point. The critical transition point is then shifted with the active state only being present for values of the branching greater than some positive critical value (as indicated in Figure 5b). Consequently, we see that there is a second critical dimension $d'_c \approx 4/3$ whose presence immediately rules out any possibility of accessing the non-trivial behavior expected in $d = 1$ via perturbative epsilon expansions down from $d = 2$. Instead cruder techniques (such as the loop expansion in fixed dimension) must be employed.⁹

We now review the effects of introducing a surface into the BARW universality class²⁷ and further allow for the possibility of a symmetry-breaking $A \rightarrow \emptyset$ reaction to take place (with rate μ_s), but only on the surface.

8.3. $\mu_s = 0$ BARW field theory

In this case only the branching process is relevant on the surface. However, as in the bulk, one must still be careful to include the surface branching processes generated by a combination of branching and annihilation. This leads to a full surface action of the form

$$S_{\text{surface}} = \int d^{d-1}x_{\parallel} \int_0^{\tau} dt \left(\sum_{l=1}^{m/2} \sigma_{2l_s} (1 - \hat{\psi}_s^{2l}) \hat{\psi}_s \psi_s \right), \quad (54)$$

where $\hat{\psi}_s = \hat{\psi}(\mathbf{x}_{\parallel}, x_{\perp} = 0, t)$ and $\psi_s = \psi(\mathbf{x}_{\parallel}, x_{\perp} = 0, t)$. Notice that the parity symmetry (53) is preserved for the $\mu_s = 0$ model at the wall, as well as in the bulk. This boundary action leads to boundary conditions very similar to those discussed earlier for DP, of the form $D\partial_{x_{\perp}}\psi|_{x_{\perp}} = \Delta_s\psi_s$, where Δ_s is the surface mass, equal to $-m\sigma_{m_s}$ in mean field theory.

Power counting on the above action reveals that the surface branching rates σ_{2l_s} all have naive dimension $[\sigma_{2l_s}] \sim \kappa^1$, where κ denotes an inverse length scale. However, close to, but below $d = 2$, this scaling dimension will be renormalized downwards (this can be seen physically as a result of processes like $A \rightarrow 3A \rightarrow A$

rendering the branching process less efficient). As a result of this renormalization, we expect the lowest generated process (i.e. with $l = 1$ in Eq. (54)) will become the *most* relevant (as it was in the bulk). Nevertheless, despite this downward renormalization, close enough to $d = 2$, the scaling dimension of the most relevant coupling σ_{2_s} will remain positive, and thus it will flow to ∞ for all nonzero starting values. This state of affairs corresponds to the extraordinary transition, where the surface is *active* while the bulk is critical. On the other hand, at bulk criticality and with $\sigma_{2_s} = 0$, we have a multicritical special transition point. Hence, for $\mu_s = 0$ and close to $d = 2$ the basic structure of the phase diagram is unchanged from mean field theory, although the values of the exponents will of course be altered by the fluctuations. In this case, after writing down and solving the appropriate RG equations (exactly along the lines of Refs. 9,16), one can derive scaling results for the density similar to those quoted in Section 7.3.

The situation in $d = 1$ is rather different, partly due to the shift of the bulk critical point away from $\sigma_m = 0$. This ensures that the boundary and bulk transitions in $d = 1$ are inaccessible to controlled perturbative expansions. Nevertheless we still expect the scaling dimension of all the σ_{2l_s} to be negative in $d = 1$, following the downwards trend in the renormalization mentioned above. In that case surface branching is then *irrelevant* in $d = 1$ leading to the Sp^* and Sp special transitions discussed earlier. Hence, if the above scenario is correct, we do not expect to see an extraordinary transition in $d = 1$ for any finite value of the surface branching, since the surface branching will always be irrelevant. This conclusion was investigated numerically in Ref. 27, where no evidence of an active surface state for $\sigma_m \leq \sigma_{m,\text{critical}}$ was found even for very high values of the surface branching parameter in a fermionic lattice model in $d = 1$.

8.4. $\mu_s \neq 0$ BARW field theory

In this case the reaction $A \rightarrow \emptyset$ is now possible, but only at sites on the wall. Including surface processes generated by a combination of branching and annihilation (i.e. the processes $A \rightarrow mA$, $A \rightarrow (m-1)A$, \dots , $A \rightarrow 2A$), the full surface action becomes

$$S_2 = \int d^{d-1}x_{\parallel} \int_0^{\tau} dt \left(\sum_{l=1}^m \sigma_{l_s} (1 - \hat{\psi}_s^l) \hat{\psi}_s \psi_s + \mu_s (\hat{\psi}_s - 1) \psi_s \right). \quad (55)$$

Note that the symmetry (53) is now broken by the surface term proportional to μ_s , which describes the $A \rightarrow \emptyset$ reaction. Once again we have a boundary condition of the form $D\partial_{x_{\perp}}\psi|_{x_{\perp}} = \Delta_s\psi_s$, where now $\Delta_s = -m\sigma_{m_s} + \mu_s$ in mean field theory.

The renormalization of the action (55) is now somewhat different from the $\mu_s = 0$ case. We again expect that we need only keep the lowest generated branching term on the surface, namely that with $l = 1$ in Eq. (55). As before, we expect fluctuations to lower the scaling dimension of this coupling from its mean field value (although actually in $d = 2$ this suppression will only be logarithmic). On the other hand, the efficacy of the $A \rightarrow \emptyset$ reaction is certainly *not* reduced by fluctuations. Hence,

for $d \leq 2$, we expect that $\Delta_s \sim \mu_s - \sigma_{1_s}$ will always run to the fixed point at ∞ , corresponding to the ordinary transition. In particular we expect this picture to also hold in $d = 1$, although in that case the transition at $\sigma_m = \sigma_{m,\text{critical}}$ will not be accessible to controlled perturbative expansions. In $d = 1$ we therefore expect to find the O^* ($\sigma_m < \sigma_{m,\text{critical}}$) or O ($\sigma_m = \sigma_{m,\text{critical}}$) transitions mentioned earlier. Hence we find a state of affairs very different from mean field theory: fluctuation effects now ensure that only the ordinary transition is accessible for $d \leq 2$, when $\mu_s > 0$.

9. Exact Results

In the last section we reviewed the use of field theoretic methods to understand the effects of fluctuations in the boundary DP and BARW models. Unfortunately, for the case of BARW, the presence of a second critical dimension d'_c prevents a controlled, perturbative investigation of the system in $d = 1$. Hence, given the fundamental difficulties associated with the BARW field theory, it seems fruitful to search for alternative approaches. One such alternative is provided by the theory of quantum spin Hamiltonians to which we now turn.

The methods we review, first presented in Ref. 27, are a straightforward extension of the work in Refs. 36 and 56. The starting point is the following set of rules for BARW with $m = 2$ in $d = 1$:

$$\begin{aligned}
 \emptyset A &\leftrightarrow A \emptyset && \text{with rate } D/2 \\
 AA &\rightarrow \emptyset \emptyset && \text{with rate } \lambda \\
 \emptyset A \emptyset &\leftrightarrow AAA \text{ and } \emptyset AA \leftrightarrow AA \emptyset && \text{with rate } \alpha/2.
 \end{aligned}
 \tag{56}$$

Note that these rules are fermionic in character (no more than one particle per site is permitted) in contrast to the bosonic rules employed in the derivation of the earlier field theories.⁵⁵ The model described in Eq. (56) can be transformed into a spin picture by writing the configuration of a semi-infinite system as a vector $|s_1, s_2, s_3, \dots\rangle$, where $s_i = 1/2$ if the i -th site is empty, and $s_i = -1/2$ if that site is occupied. Hence the system ket is given by

$$|P(t)\rangle = \sum_{\{s_i\}} P(\{s_i\}; t) |\{s_i\}\rangle,
 \tag{57}$$

and the equation governing the time evolution is

$$\partial_t |P(t)\rangle = -\mathcal{H} |P(t)\rangle,
 \tag{58}$$

where, using a representation in terms of Pauli matrices, and defining $n_k = (1 - \sigma_k^z)/2$, $v_k = 1 - n_k$, $s_k^\pm = (\sigma_k^x \pm i\sigma_k^y)/2$, we have³⁶

$$\mathcal{H} = \frac{1}{2} \sum_{k=1}^{\infty} (D[n_k v_{k+1} + v_k n_{k+1} - s_k^+ s_{k+1}^- - s_k^- s_{k+1}^+])$$

$$\begin{aligned}
 & + 2\lambda[n_k n_{k+1} - s_k^+ s_{k+1}^+] + \frac{\alpha}{2} \sum_{k=2}^{\infty} (1 - \sigma_{k-1}^x \sigma_{k+1}^x) n_k \\
 & = DH^{\text{SEP}} + \lambda H^{\text{RSA}} + \alpha H^{\text{BARW}} \\
 & = D \sum_{k=1}^{\infty} h_k^{\text{SEP}} + \lambda \sum_{k=1}^{\infty} h_k^{\text{RSA}} + \alpha \sum_{k=2}^{\infty} h_k^{\text{BARW}}.
 \end{aligned} \tag{59}$$

Here we have used some of the notation of Ref. 36, where SEP (symmetric exclusion process) refers to the diffusion piece, RSA (random-sequential adsorption) to the annihilation piece and BARW to the branching piece of the “quantum Hamiltonian”. Notice that the boundary has been included in Eq. (59), since particles may not hop to the left of site 1, and the annihilation/branching processes have also been restricted to sites $1, 2, 3, \dots$. Hence, the above operator \mathcal{H} governs the evolution of a $d = 1$ BARW system *without* an $A \rightarrow \emptyset$ reaction at the boundary. Averages are calculated using the projection state $\langle | = \sum_{\{s_i\}} \langle \{s_i\} |$, i.e. $\langle \mathcal{F} \rangle = \langle | \mathcal{F} | P(t) \rangle$. Following Ref. 36, we now define an operator \mathcal{D} where

$$\mathcal{D} = \gamma_{-1} \gamma_0 \gamma_1 \gamma_2 \dots, \tag{60}$$

with

$$\begin{aligned}
 \gamma_{2k-1} &= \frac{1}{2} [(1+i)\sigma_k^z - (1-i)], \\
 \gamma_{2k} &= \frac{1}{2} [(1+i)\sigma_k^x \sigma_{k+1}^x - (1-i)].
 \end{aligned} \tag{61}$$

Defining a new “quantum Hamiltonian” as $\tilde{\mathcal{H}} = [\mathcal{D}^{-1} \mathcal{H} \mathcal{D}]^T$, we find

$$\begin{aligned}
 \tilde{\mathcal{H}} &= (D - \lambda) \sum_{k=1}^{\infty} h_k^{\text{BARW}} + (\alpha + \lambda) \sum_{k=1}^{\infty} h_k^{\text{SEP}} + \lambda \sum_{k=1}^{\infty} h_k^{\text{RSA}} \\
 &+ \frac{\lambda}{2} (n_1 n_0 - s_1^+ s_0^+ + n_1 v_0 - s_1^+ s_0^-),
 \end{aligned} \tag{62}$$

where we have used the commutation rules described in detail in Ref. 36. Hence, when $D = \lambda + \alpha$, we have the following processes occurring:

$$\begin{aligned}
 \emptyset_i A_{i+1} &\leftrightarrow A_i \emptyset_{i+1} & \text{rate } (\lambda + \alpha)/2, & \quad i = 1, 2, 3, \dots, \\
 A_i A_{i+1} &\rightarrow \emptyset_i \emptyset_{i+1} & \text{rate } \lambda, & \quad i = 1, 2, 3, \dots, \\
 \emptyset_{i-1} A_i \emptyset_{i+1} &\leftrightarrow A_{i-1} A_i A_{i+1} & \text{rate } \alpha/2, & \quad i = 1, 2, 3, \dots, \\
 \emptyset_{i-1} A_i A_{i+1} &\leftrightarrow A_{i-1} A_i \emptyset_{i+1} & \text{rate } \alpha/2, & \quad i = 1, 2, 3, \dots, \\
 A_0 A_1 &\rightarrow \emptyset_0 \emptyset_1 & \text{rate } \lambda/2, & \\
 \emptyset_0 A_1 &\rightarrow A_0 \emptyset_1 & \text{rate } \lambda/2. &
 \end{aligned} \tag{63}$$

Excepting the boundary terms, we see that the Hamiltonian has been mapped back onto itself. Furthermore, at the edge, the particles may only hop from site 1 to site 0 but never the other way round. This means that we can forget about the 0-th site

in exchange for allowing the processes $A_1 A_2 \leftrightarrow A_1 \emptyset_2$ (with rate $\alpha/2$), and $A_1 \rightarrow \emptyset_1$ (with rate $\lambda/2$). Hence, we see that the new Hamiltonian $\tilde{\mathcal{H}}$ corresponds to the case where $\mu_s \neq 0$, with the DP processes $A \leftrightarrow A + A$ and $A \rightarrow \emptyset$ generated on the boundary.

If we choose the initial condition to be an uncorrelated state with density $1/2$, denoted by $|1/2\rangle$, then the density at site k , $\rho_k(t)$, is given by

$$\rho_k(t) = \langle |n_k \exp(-\mathcal{H}t) |1/2\rangle. \quad (64)$$

Following exactly the procedure in Refs. 36 and 56 (starting with insertions of the identity operator $\mathcal{D}\mathcal{D}^{-1}$ into the RHS of Eq. (64)), one can straightforwardly show that

$$\rho_k(t) = \frac{1}{2}[1 - \langle 0 | \exp(-\tilde{\mathcal{H}}t) |k-1, k\rangle], \quad (65)$$

where $\langle 0 |$ is the vacuum state (with no particles), and $|k-1, k\rangle$ is the initial state with only two particles situated at sites $k-1$ and k . In Eq. (65) the LHS is the density at the k -th site, whereas the RHS is one-half times the probability that a cluster initiated at $t=0$ by two particles at sites $k-1$ and k has not yet died out by time t . According to our earlier analysis, for $\Delta < 0$, the LHS should scale as $|\Delta|^{\beta_{\text{dens}}}$ (far from the wall) or $|\Delta|^{\beta_{1,\text{dens}}^{\text{Sp}}}$ (close to the wall), and the RHS as $|\Delta|^{\beta_{\text{seed}}}$ (far from the wall) or $|\Delta|^{\beta_{1,\text{seed}}^{\text{O}}}$ (close to the wall). Thus, at the line $D = \lambda + \alpha$, we have proven the result

$$\beta_{1,\text{seed}}^{\text{O}} = \beta_{1,\text{dens}}^{\text{Sp}} \quad (66)$$

(and, of course, the bulk result $\beta_{\text{seed}} = \beta_{\text{dens}}$). We note that the bulk result was first proven in Ref. 36, and a very similar result for the $A + A \rightarrow \emptyset$ reaction was derived in Ref. 56 (connecting the O* and Sp* regimes). Using universality, it was postulated in Ref. 27 that this equality between the two surface exponents is valid everywhere close to the transition line, and not just where $D = \lambda + \alpha$.

At the line $D = \lambda + \alpha$, it is now straightforward to derive a second relation

$$\beta_{1,\text{seed}}^{\text{Sp}} = \beta_{1,\text{dens}}^{\text{O}}. \quad (67)$$

One simply starts off with the quantum Hamiltonian $\tilde{\mathcal{H}}$ and then follows the same steps as above. $\tilde{\mathcal{H}}$ can then be mapped back onto the starting Hamiltonian \mathcal{H} , meaning that the transformation is actually a duality transformation. A relation like that in Eq. (65) can then be derived, giving the above result.

In summary, in $d = 1$ and at the particular line in parameter space $D = \lambda + \alpha$, we have mapped BARW at the special transition onto BARW at the ordinary transition (and vice-versa), a rather non-trivial procedure reminiscent of a related transformation in the Ising model. Unfortunately, the results (66) and (67) are only derived for one line in parameter space and we have to rely on universality in order to claim that they are valid elsewhere close to the transition line.

10. Numerical Methods

We now discuss the various numerical methods which can be used to obtain precise estimates for the critical exponents for boundary DP and BARW. The values of the exponents are listed in Section 10.3.

10.1. Extraction of exponents from Monte-Carlo simulations

In this subsection we review how the exponents are extracted from Monte-Carlo simulation data for the DP and DP2 models with walls in $d = 1$ and $d = 2$.^{18,19,21,27} Numerics have also been carried out for BARW with a wall in $d = 1$, with results in good agreement with boundary DP2 simulations.²⁷ The most efficient way of extracting information on boundary DP and DP2 is to perform simulations at criticality, starting from an initial seed next to the wall. Measurements can then be taken of the survival probability $P_1(t)$, the activity in the bulk $N_1(t)$ and at the wall $N_{1,1}(t)$, the average spread of the cluster $\langle x^2(t) \rangle$, and the probability $p_1(s)$ to have a cluster of size (mass) s .³⁵ Furthermore, by averaging over surviving clusters only (denoted by an over-line), measurements can be taken of the surviving bulk activity $\overline{N_1}(t)$ and the surviving wall activity $\overline{N_{1,1}}(t)$. Although carrying out these simulations is straightforward, extracting the exponents discussed in the previous sections requires some further analysis. We will now review the scaling theory which allows these connections to be made.⁵⁷ Note that all the relations given below are valid for the DP ordinary transition and for both the IBC (special) and RBC (ordinary) DP2 transitions, and hence these labels will be suppressed from now on.

The probability for a cluster grown from a seed on the wall still to be alive at time t is given by Eqs. (24) and (37). At criticality ($\Delta = 0$) it has the following behavior

$$P_1(t) = t^{-\delta_{1,\text{seed}}} f(t/t_c), \quad \delta_{1,\text{seed}} = \beta_{1,\text{seed}}/\nu_{\parallel}, \quad (68)$$

where the scaling function f depends on the cutoff $t_c \sim \xi_{\parallel} \sim |\Delta|^{-\nu_{\parallel}}$. Hence, the probability of growing a cluster which lives exactly t time steps behaves as $p_1(t) \sim t^{-1-\delta_{1,\text{seed}}}$.

The average number of active sites at criticality, averaged over all clusters, is obtained by integrating the density (27) and (38) over space, giving

$$N_1(t) \sim t^{\kappa_1}, \quad \kappa_1 = d\chi - \delta_{\text{dens}} - \delta_{1,\text{seed}}, \quad (69)$$

where we have introduced the cluster envelope or “roughness” exponent $\chi = \nu_{\perp}/\nu_{\parallel}$ ($\equiv 1/z$), and the notation $\delta_{\text{dens}} = \beta_{\text{dens}}/\nu_{\parallel}$. Note that the scaling relation in Eq. (69) corresponds to the hyperscaling relations (30) and (41), a fact which follows from $\langle s_1(t) \rangle = \int_0^t dt' N_1(t')$, and the relation $\gamma_1 = \nu_{\parallel}(1 + \kappa_1)$. By integrating the density on the wall (28) and (39), we obtain the average number of active sites at criticality on the wall

$$N_{1,1}(t) \sim t^{\kappa_{1,1}}, \quad \kappa_{1,1} = (d-1)\chi - \delta_{1,\text{dens}} - \delta_{1,\text{seed}}, \quad (70)$$

where $\delta_{1,\text{dens}} = \beta_{1,\text{dens}}/\nu_{\parallel}$. Note also that the scaling relation in Eq. (70) corresponds to the hyperscaling relations (33) and (43) at criticality, since $\langle s_{1,1}(t) \rangle = \int_0^t dt' N_{1,1}(t')$, and $\gamma_{1,1} = \nu_{\parallel}(1 + \kappa_{1,1})$.

Alternatively, by averaging only over clusters which survive to infinity (denoted by an over-line), we obtain

$$\overline{N_1}(t) \sim t^{\overline{\kappa_1}}, \quad \overline{\kappa_1} = d\chi - \delta_{\text{dens}}. \tag{71}$$

The activity on the wall for surviving clusters reads

$$\overline{N_{1,1}}(t) \sim t^{\overline{\kappa_{1,1}}}, \quad \overline{\kappa_{1,1}} = (d - 1)\chi - \delta_{1,\text{dens}}. \tag{72}$$

Simulations in $d = 1$ thus directly yield $\delta_{1,\text{dens}}$. The average position of activity follows from Eqs. (27) and (38), giving $\langle x^2 \rangle \sim t^{2\chi}$, where x is the distance from the seed and the average is taken over all active points at a given time.

Additional numerical data was obtained in Refs. 21,27 by considering the cluster size distributions at criticality. In the bulk the typical cluster size s_c of finite clusters scales as volume times density, i.e.,

$$s_c \sim \xi_{\perp}^d \xi_{\parallel} n(\Delta) \sim |\Delta|^{-1/\sigma}, \quad 1/\sigma = d\nu_{\perp} + \nu_{\parallel} - \beta_{\text{dens}}. \tag{73}$$

From the lifetime survival distribution (68), it is then straightforward to obtain the probability $P_1(s)$ to have a cluster of size larger than s , for clusters started from a seed on the wall. Using the fact that the lifetime is set by the parallel correlation length, $t \sim \xi_{\parallel} \sim |\Delta|^{-\nu_{\parallel}}$, we see that the typical cluster size and lifetime are connected by $s \sim t^{1/\nu_{\parallel}\sigma}$. Hence we obtain $P_1(s) \sim P_1(t \sim s^{\nu_{\parallel}\sigma}) \sim s^{-\beta_{1,\text{seed}}\sigma}$. Thus, we eventually obtain the probability $p_1(s)$ to have a cluster of exactly size s , $p_1(s) = -dP_1(s)/ds$, with the result

$$p_1(s) = s^{-\mu_1} g(s/s_c), \quad \mu_1 = 1 + \frac{\beta_{1,\text{seed}}}{d\nu_{\perp} + \nu_{\parallel} - \beta_{\text{dens}}}. \tag{74}$$

Similarly, the cluster size distribution on the wall due to a seed located at the wall can also be obtained. In this case the typical cluster size of finite clusters is

$$s_{\text{wall},c} \sim \xi_{\perp}^{d-1} \xi_{\parallel} n_1(\Delta) \sim |\Delta|^{-1/\sigma_1}, \tag{75}$$

where the cutoff exponent is

$$1/\sigma_1 = (d - 1)\nu_{\perp} + \nu_{\parallel} - \beta_{1,\text{dens}}. \tag{76}$$

The resulting distribution reads

$$p_{1,1}(s_{\text{wall}}) = s_{\text{wall}}^{-\mu_{1,1}} f(s_{\text{wall}}/s_{\text{wall},c}), \tag{77}$$

with

$$\mu_{1,1} = 1 + \frac{\beta_{1,\text{seed}}}{(d - 1)\nu_{\perp} + \nu_{\parallel} - \beta_{1,\text{dens}}}. \tag{78}$$

With the above scaling relations it is now straightforward to extract all the exponents from the numerical data. Values for the exponents obtained in this way are listed in Section 10.3. An additional interesting exponent relation for the RBC transition for DP2 can be obtained by assuming that the survival probability is dominated by the return to the wall of the cluster-envelope. This leads to¹⁸

$$\delta_{1,\text{seed}}^{\text{RBC}} = 1 - \chi, \quad (79)$$

in agreement with the simulation results for the RBC (see Section 10.3). Qualitatively, this means that the I_2 regions located at the wall determine the scaling since they can only disappear when the activity returns to the wall. Note that a relation of this kind clearly fails for the IBC transition. Furthermore, if the cluster lifetime is defined to be the return time of the cluster-envelope (i.e. the return time of the rightmost active site) to the initial point, then we expect clusters defined in this way to have a lifetime distribution exponent $\delta_{1,\text{seed}}$ given by Eq. (79). This prediction is in agreement with the simulations in Ref. 12, where various models in the DP and BARW classes were studied with cluster lifetimes defined in the way described above. For further information on the DP2 boundary exponents, including inequalities for the $\beta_{1,\text{seed}}$ and $\beta_{1,\text{dens}}$ exponents, we refer to Ref. 27.

10.2. Series expansions

In the previous subsection we reviewed the scaling relations used to extract exponents from Monte-Carlo simulations. These simulations provide fairly accurate exponent estimates for both the DP and BARW classes (see the next subsection). However, for the case of DP in $d = 1$ (but curiously *not* for BARW in $d = 1$ ⁴⁵) this level of accuracy can be far surpassed by using the method of series expansions.^{17,22} With uncertainties in the seventh or eighth digit, these exponent values are very reliable and useful for testing conjectures and scaling laws. For example, most of the DP exponents in $d = 1$ are now known not to lie close to any simple rational numbers. In fact, it seems more likely that the exponents are irrational. However, one important exception is the exponent τ_1 governing the mean cluster lifetime in the presence of a wall (see Eq. (25)). This exponent has been conjectured to equal unity,¹⁷ although this has now been challenged by the estimate $\tau_1 = 1.00014(2)$ (see below).²²

The idea behind series expansions in DP is to find an effective algorithm for calculating the expansion coefficients of moments of the pair-connectedness (the probability that the site x at time t is occupied given a seed at the origin at $t = 0$). By analyzing these expansions, critical parameters of the model can be obtained, including estimates for p_c , and the exponents γ , ν_\perp , and ν_\parallel . These series expansions can be generated by transfer matrices that relate states at time t to those at one time step later. At any time t this gives polynomials in the percolation probability p . Since the difficulty in generating these series expansions is of exponential complexity, a large amount of effort has been devoted to keeping the computational effort as small as possible (see Ref. 44 and references therein). Once a series expansion is

derived, it is then analyzed by using differential approximants. The more terms that can be computed in the series, the more accurately the exponents can be estimated.

10.3. Exponent Values

In this section we list the best exponent values currently available for the surface and bulk exponents for DP and BARW. As we have mentioned, for DP in $d = 1$ the best results are from series expansions; in all other cases we give Monte-Carlo data. Note that various attempts have been made to fit these exponent values with rational numbers; further details can be found in Refs. 17,27.

Table 4. Critical exponents for DP in $d = 1$ and $d = 2$ in the bulk and for the ordinary transition at the boundary.

	$d = 1$	$d = 2$	Mean Field
$\delta_{\text{dens}} = \delta_{\text{seed}}$	0.159 464(6)	0.450(1)	1
$\delta_{1,\text{dens}} = \delta_{1,\text{seed}}$	0.423 17(2)	0.82(4)	3/2
κ	0.313 686(8)	0.230(1)	0
κ_1	0.049 98(2)	-0.13(1)	-1/2
$\bar{\kappa} = \overline{\kappa_1}$	0.473 150(10)	0.682(1)	1
μ	1.108 247(10)	1.268(8)	3/2
μ_1	1.287 25(2)	1.49(8)	7/4
2χ	1.265 226(13)	1.132(7)	1
$\beta_{\text{dens}} = \beta_{\text{seed}}$	0.276 486(8)	0.583(4)	1
$\beta_{1,\text{dens}} = \beta_{1,\text{seed}}$	0.733 71(2)	1.07(5)	3/2
τ	1.457 362(14)	0.711(7)	0
τ_1	1.000 14(2)	0.26(2)	0
γ	2.277 730(5)	1.593(7)	1
γ_1	1.820 51(1)	1.05(2)	1/2

Table 5. Critical exponents for the BARW class measured from simulations of DP2 in $d = 1$.

	$d = 1$	$d = 1$ (IBC)	$d = 1$ (RBC)
δ_{dens}	0.287(5)	0.288(2)	0.291(4)
δ_{seed}	0.290(5)		
$\delta_{1,\text{seed}}$		0.641(2)	0.426(3)
$\delta_{1,\text{dens}}$		0.415(3)	0.635(2)
κ	0.000(2)		
κ_1		-0.354(2)	-0.141(2)
$\bar{\kappa} = \overline{\kappa_1}$	0.288(5)	0.287(2)	0.285(2)
μ	1.225(5)		
μ_1		1.500(3)	1.336(3)
$\mu_{1,1}$	1.408(5)	2.05(5)	2.15(5)
2χ	1.150(5)	1.150(3)	1.152(3)
β_{dens}	0.922(5)	0.93(1)	0.94(2)
β_{seed}	0.93(5)		
$\beta_{1,\text{seed}}$		2.06(2)	1.37(2)
$\beta_{1,\text{dens}}$		1.34(2)	2.04(2)
τ	2.30(3)		
τ_1		1.16(4)	1.85(4)
γ	3.22(5)		
γ_1		2.08(4)	2.77(4)
$\gamma_{1,1}$	1.38(3)	(< 0)	(< 0)

11. Other Directions

In this section we briefly mention some other nonequilibrium systems where boundary effects have been analyzed. Additional studies, which we will not discuss, include (i) the connection between surface DP and local persistence;²⁰ (ii) $d = 1$ density matrix renormalization group calculations of some reaction-diffusion processes;²⁴ (iii) active, but slanted, walls in DP, which give rise to a “curtain” of activity whose width is given by an angle-dependent correction to bulk DP;²⁵ and, finally, (iv) Monte-Carlo simulation studies of rigidity percolation with and without walls, which have shown the model to belong to the DP universality class.²³

11.1. Compact DP

By forcing a DP cluster to be dense one obtains a different universality class called Compact Directed Percolation.³² This actually corresponds to the special case $q = 1$ of the Domany-Kinzel model in Figures 1 and 2. The constraint $q = 1$ forces all interior sites and/or bonds to be active, whereas the size of the cluster is controlled by p , which now only affects the boundaries of the cluster. As the dynamics of the cluster is entirely controlled by the dynamics of its surface, the problem is greatly simplified. For instance, in $d = 1$, the extinction of a compact DP cluster can be viewed as the probability for a pair of random walkers to coincide. It is therefore no surprise that compact DP can be exactly solved in $d = 1$ and that all the exponents are simple integers.³² For bulk compact DP in $d = 1$, one has $\beta_{\text{seed}} = 1$, $\nu_{\parallel} = 2$, $\nu_{\perp} = 1$, and $\gamma = 2$.

By introducing a wall in compact DP, the survival probability is altered and one obtains surface critical exponents just as for DP. With an *inactive wall*, the cluster is free to approach and leave the wall, but not cross. For $d = 1$, this gives rise to $\beta_{1,\text{seed}} = 2$, i.e., twice as big as β_{seed} for the bulk.^{58,59} On the other hand, for an *active wall*, the cluster is stuck to the wall and therefore described by a single random walker for $d = 1$. By reflection in the wall, this may be viewed as *symmetric* compact DP which has the same β_{seed} as normal compact DP, giving $\beta_{1,\text{seed}} = 1$.⁶⁰

11.2. Backbone and red bonds in DP

In Ref. 18 the so-called backbone and red bonds of $d = 1$ DP clusters have been investigated. The backbone is obtained from the infinite cluster by removing all dangling ends. Thus the backbone consists of precisely those bonds which would be occupied by both the time-directed DP process and its reverse time-directed process. It then follows that the backbone density $|\Delta|^{\beta^{BB}}$ is described by the exponent $\beta^{BB} = 2\beta$. Numerically, the backbone dimension on the wall was measured with the result $D_1^{BB} = 0.16 \pm 0.01$. Using the scaling relation $D_1^{BB} = 1 - \beta_1^{BB}/\nu_{\parallel}$ it then follows that $\beta_1^{BB} = 1.46$ in good agreement with $\beta_1^{BB} = 2\beta_1$, cf. the result for the bulk.

On the backbone one can identify so-called red bonds⁶¹ that, if one is cut, divide the cluster into two parts. A renormalization group argument⁶² (see also Ref. 63)

yields that the number of red bonds up to time t scales as

$$N_R(t) \sim t^{1/\nu_{\parallel}}. \quad (80)$$

Reference 18 measured the scaling of red bonds for DP with a wall and obtained results in complete agreement with Eq. (80). In addition the scaling of red bonds along a longitudinal cut for DP with no wall was measured with the result $N_R^{cut}(t) \sim t^{-0.04 \pm 0.02}$. This is in accordance with the expected behavior $N_R^{cut}(t) \sim t^{1/\nu_{\parallel} - \nu_{\perp}/\nu_{\parallel}} \sim t^{-0.056}$, where the extra factor originates from the scaling of the width $\xi_{\perp} \sim t^{\nu_{\perp}/\nu_{\parallel}}$ of the cluster. Finally, the scaling of boundary red bonds for DP with the wall was measured, where the behavior $N_{R,1}(t) \sim t^{-0.60 \pm 0.1}$ was found.

11.3. Invasion Percolation

Finally, we briefly discuss a slightly different system, namely invasion percolation (IP), which is a model for the growth of infinite percolation clusters at criticality.⁶⁴ In $d = 2$ the fractal dimension of IP clusters is $D = 2 - \beta/\nu = 2 - (5/36)/(4/3) = 91/48 \approx 1.90$, where the known exact values for percolation in $d = 2$ have been used (see, e.g., Ref. 65).

In Ref. 66, boundary effects in the growth of $d = 2$ invasion percolation clusters were studied. Numerically, near a wall it was found that the fractal dimension of IP clusters was $D_s = 1.67 \pm 0.03$. Using the scaling theory for boundary nonequilibrium systems, it follows that the activity on the wall has the fractal dimension $D_1 = 1 - \beta_1/\nu$, where β_1 is the surface exponent for $d = 2$ percolation. Using $\beta_1 = 4/9$, we obtain that $D_1 = 2/3$. The fractal dimension of parts of the cluster close to the wall is thus predicted to be $D_1 + 1 = 5/3$ in excellent agreement with the simulation result.

12. Summary

In this review we have outlined the boundary critical behavior of some nonequilibrium systems, with a particular focus on the directed percolation and branching-annihilating random walk universality classes. Through the use of a variety of theoretical and numerical techniques, including mean field, scaling and field theories, exact solutions, Monte-Carlo simulations, and series expansions, a considerable amount of progress has been made in understanding the boundary critical properties of these models. Nevertheless some important problems remain open and we wish to conclude this review with a brief list of some of these remaining questions.

1. Due to the presence of a second critical dimension d'_c , the BARW field theory in $d = 1$ is not well-controlled either at the boundary or in the bulk. An improved theory would be highly desirable in confirming the results provided by exact solutions and Monte-Carlo simulations.

2. Although we have not discussed it in this review, the boundary critical properties of *dynamical percolation* form another interesting case (for $d \geq 2$).²⁸ In this

universality class the development of an appropriate boundary field theory, and the calculation of boundary exponents using epsilon expansion techniques, has not yet been attempted.

3. The intriguing question of whether $\tau_1 = 1$ for the DP ordinary transition in $d = 1$ remains unsolved. No theoretical explanation has emerged for why τ_1 should equal unity, and, in fact, the latest series expansions yield a value for τ_1 very slightly away from $\tau_1 = 1$. Hence the possibility of numerical coincidence, where τ_1 just happens to lie very close to unity, cannot be ruled out.

4. Most of the numerical work so far has focused on the ordinary transition. Particularly for the case of DP, it would be useful to measure the exponents at the extraordinary and special transitions for $d > 1$.

Acknowledgements

Part of this work was carried out while M.H. and K.B.L. were at the Niels Bohr Institute. P.F. acknowledges support from the Swedish Natural Science Research Council. M.H. acknowledges support from the CATS group at the Niels Bohr Institute, from the NSF through the Division of Materials Research and from NSERC of Canada. K.B.L. acknowledges support from the Carlsberg Foundation.

References

1. K. Binder, in *Phase Transitions and Critical Phenomena*, Vol. 8, edited by C. Domb and J. L. Lebowitz (Academic Press, London, 1983).
2. H. W. Diehl, in *Phase Transitions and Critical Phenomena*, Vol. 10, edited by C. Domb and J. L. Lebowitz (Academic Press, London, 1986).
3. H. W. Diehl, *Int. J. Mod. Phys. B* **11**, 3593 (1997).
4. W. Kinzel, in *Percolation Structures and Processes*, edited by G. Deutscher, R. Zallen, and J. Adler, *Annals of the Israel Physical Society*, Vol. 5 (Adam Hilger, Bristol, 1983).
5. R. Dickman, in *Nonequilibrium Statistical Mechanics in One Dimension*, ed. V. Privman (Cambridge University Press, Cambridge, 1997).
6. H. Hinrichsen, *Adv. Phys.* **49**, 815 (2000).
7. H. Takayasu and A. Yu. Tretyakov, *Phys. Rev. Lett.* **68**, 3060 (1992).
8. I. Jensen, *Phys. Rev. E* **50**, 3623 (1994).
9. J. Cardy and U. C. Täuber, *Phys. Rev. Lett.* **77**, 4780 (1996); *J. Stat. Phys.* **90**, 1 (1998).
10. P. Grassberger, F. Krause, and T. von der Twer, *J. Phys. A: Math. Gen.* **17**, L105 (1984); P. Grassberger, *J. Phys. A: Math. Gen.* **22**, L1103 (1989).
11. M. H. Kim and H. Park, *Phys. Rev. Lett.* **73**, 2579 (1994); H. Park, M. H. Kim, and H. Park, *Phys. Rev. E* **52**, 5664 (1995).
12. W. Hwang, S. Kwon, H. Park, and H. Park, *Phys. Rev. E* **57**, 6438 (1998).
13. W. Hwang and H. Park, *Phys. Rev. E* **59**, 4683 (1999).
14. N. Menyhárd and G. Ódor, *J. Phys. A* **29**, 7739 (1996).
15. H. Hinrichsen, *Phys. Rev. E* **55**, 219 (1997).
16. H. K. Janssen, B. Schaub, and B. Schmittmann, *Z. Phys. B* **72**, 111 (1988).

17. J. W. Essam, A. J. Guttmann, I. Jensen, and D. TanlaKishani, *J. Phys. A* **29**, 1619 (1996).
18. K. B. Lauritsen, K. Sneppen, M. Markošová, and M. H. Jensen, *Physica A* **247**, 1 (1997).
19. P. Fröjdh, M. Howard, and K. B. Lauritsen, *J. Phys. A* **31**, 2311 (1998).
20. H. Hinrichsen and H. M. Koduvely, *Eur. Phys. J. B* **5**, 257 (1998).
21. K. B. Lauritsen, P. Fröjdh, and M. Howard, *Phys. Rev. Lett.* **81**, 2104 (1998).
22. I. Jensen, *J. Phys. A* **32**, 6055 (1999).
23. M. A. de Menezes and C. F. Moukarzel, *Phys. Rev. E* **60**, 5699 (1999).
24. E. Carlon, M. Henkel, and U. Schollwöck, *Eur. Phys. J. B* **12**, 99 (1999).
25. C.-C. Chen, H. Park, and M. den Nijs, *Phys. Rev. E* **60**, 2496 (1999).
26. M. J. E. Richardson and Y. Kafri, *Phys. Rev. E* **59**, R4725 (1999); Y. Kafri and M. J. E. Richardson, *J. Phys. A* **32**, 3253 (1999).
27. M. Howard, P. Fröjdh, and K. B. Lauritsen, *Phys. Rev. E* **61**, 167 (2000).
28. P. Grassberger, *J. Phys. A* **25**, 5867 (1992).
29. J. L. Cardy and R. L. Sugar, *J. Phys. A* **13**, L423 (1980).
30. H. Janssen, *Z. Phys. B* **42**, 151 (1981).
31. P. Grassberger and K. Sundermeyer, *Phys. Lett. B* **77**, 220 (1978).
32. E. Domany and W. Kinzel, *Phys. Rev. Lett.* **53**, 311 (1984).
33. W. Kinzel, *Z. Phys. B* **58**, 229 (1985).
34. Note that the convention used for Δ here is different from that in Ref. 21.
35. P. Grassberger and A. de la Torre, *Ann. Phys. (N.Y.)* **122**, 373 (1979).
36. K. Mussawisade, J. E. Santos, and G. M. Schütz, *J. Phys. A* **31**, 4381 (1998).
37. I. Jensen, *J. Phys. A* **29**, 7013 (1996).
38. J. W. Essam, K. De'Bell, J. Adler, and F. M. Bhatti, *Phys. Rev. B* **33**, 1982 (1986).
39. J. W. Essam, A. J. Guttmann, and K. De'Bell, *J. Phys. A* **21**, 3815 (1988).
40. P. Grassberger, *J. Phys. A* **22**, 3673 (1989).
41. P. Grassberger and Y.-C. Zhang, *Physica A* **224**, 169 (1996).
42. I. Jensen, *Phys. Rev. A* **45**, R563 (1992).
43. M. A. Muñoz, R. Dickman, A. Vespignani, and S. Zapperi, *Phys. Rev. E* **59**, 6175 (1999).
44. I. Jensen, *J. Phys. A* **32**, 5233 (1999).
45. I. Jensen, *J. Phys. A* **30**, 8471 (1997).
46. D. Zhong and D. ben-Avraham, *Phys. Lett. A* **209**, 333 (1995).
47. B. M. McCoy and T. T. Wu, *Phys. Rev.* **162**, 436 (1967).
48. A. J. Bray and M. A. Moore, *J. Phys. A.* **10**, 1927 (1977); T. W. Burkhardt and H. W. Diehl, *Phys. Rev. B* **50**, 3894 (1994).
49. J. L. Cardy, *Nucl. Phys. B* **240** [FS12], 514 (1984).
50. H. A. Kramers and G. H. Wannier, *Phys. Rev.* **60**, 252 (1941); *ibid.* **60**, 263 (1941).
51. A. Drewitz, R. Leidl, T. W. Burkhardt, and H. W. Diehl, *Phys. Rev. Lett.* **78**, 1090 (1997).
52. Note that the mean field surface density exponent $\beta_{1,\text{dens}}^{\text{IBC}}$ quoted in footnote [22] of Ref. 21 is incorrect.
53. J. L. Cardy, *J. Phys. A* **16**, 3617 (1983).
54. M. A. Muñoz, G. Grinstein, and Y. Tu, *Phys. Rev. E* **56**, 5101 (1997).
55. L. Peliti, *J. Physique* **46**, 1469 (1985).
56. G. M. Schütz, *Z. Phys. B* **104**, 583 (1997).
57. Note that some of our exponent definitions in this section differ from those sometimes found in the literature. In particular our κ exponents are sometimes called η , and the dynamic exponent z is sometimes redefined as $z \rightarrow 2/z$.
58. R. Bidaux and V. Privman, *J. Phys. A* **24**, L839 (1991).

59. J.-C. Lin, *Phys. Rev. A* **45**, R3394 (1992).
60. J. W. Essam and D. TanlaKishani, *J. Phys. A* **27**, 3743 (1994).
61. H. E. Stanley, *J. Phys. A* **10**, L211 (1977); R. Pike and H. E. Stanley, *ibid.* **14**, L169 (1981).
62. A. Cognilio, *Phys. Rev. Lett.* **46**, 250 (1981); *J. Phys A* **15**, 3824 (1982).
63. G. Huber, M. H. Jensen, and K. Sneppen, *Phys. Rev. E* **52**, R2133 (1995).
64. T. Vicsek, *Fractal Growth Phenomena*, 2nd ed. (World Scientific, Singapore, 1992).
65. M. Henkel, *Conformal Invariance and Critical Phenomena* (Springer-Verlag, Berlin, 1999).
66. R. Cafiero, G. Caldarelli, and A. Gabrielli, *Phys. Rev. E* **56**, R1291 (1997).